Review of upper McArthur Group stratigraphy in the Glyde Sub-basin and correlation with modern geophysical and geochemical data

Mark A. Mabarrack, BSc (University of Adelaide)

This thesis is submitted in partial fulfillment of the requirements for the
Honours Degree of Bachelor of Science (Petroleum Geology & Geophysics)
Australian School of Petroleum,
The University of Adelaide
November, 2014

Acknowledgements

Firstly, I would like to thank my industry supervisors Luke Titus and Josh Bluett from Armour Energy for making the project available. Also, for their guidance and hospitality during my industry internship at the head office in Brisbane which made understanding and starting the project an enjoyable process. I would also like to acknowledge Dr. Kathryn Amos at the Australian School of Petroleum for her assistance in the role of Academic Supervisor. Throughout the duration of the project regular meetings with Kathryn allowed for deadlines to be set and achieved. In addition to this Kathryn provided regular feedback on work and my final draft which provided me a basis to improve the quality of work I was producing. Finally, I would like to give thanks to Belinda Smith at the Northern Territory Geological Survey for her assistance with the HyLog data.

Table of Contents

1. Introduction

1.1. Location

The Glyde Sub-basin is located in the southern McArthur Basin, Northern Territory, Australia, 110 km south of Borroloola, and 80 km south of the McArthur River mine (Davidson & Dashlooty 1993; Figure 1.1). The McArthur Basin consists of the N-S trending southern Batten Fault Zone (Trough) and northern Walker Fault Zone (Trough) which are separated by the E-W trending Urapunga Fault Zone (Figure 1.1). The Glyde region (outlined in red) lies within the Batten Fault Zone and it is this area that will be the main focus of the project due to its petroleum prospectivity.

1.2. Rationale

It is the organic rich zones of the Paleoproterozoic Barney Creek Formation that are the main targets in the area for their unconventional gas potential. The reason for the interest in the region is the fact that the Barney Creek Formation is thickest in the Glyde Sub-basin with respect to the rest of the McArthur Basin (Davidson & Dashlooty 1993). Also, the Upper McArthur Group which includes the Barney Creek Formation is present at shallow depths within the region due to regional uplift, making for more cost effective drilling.

1.3. Aims and Objectives

The primary objective of the project is to make recommendations for future drilling based on the thickness and lateral extent of total organic carbon (TOC) rich zones within the Barney Creek Formation. This will be achieved by interpreting available mineral and petroleum well data to identify formations and divide them into facies based on geochemical and geophysical characteristics. In addition to this, the study will aim to re-evaluate the depositional environments of the Upper McArthur Group based on the interpretation of composite HyLog data (mineral wells) and wireline data (petroleum wells).

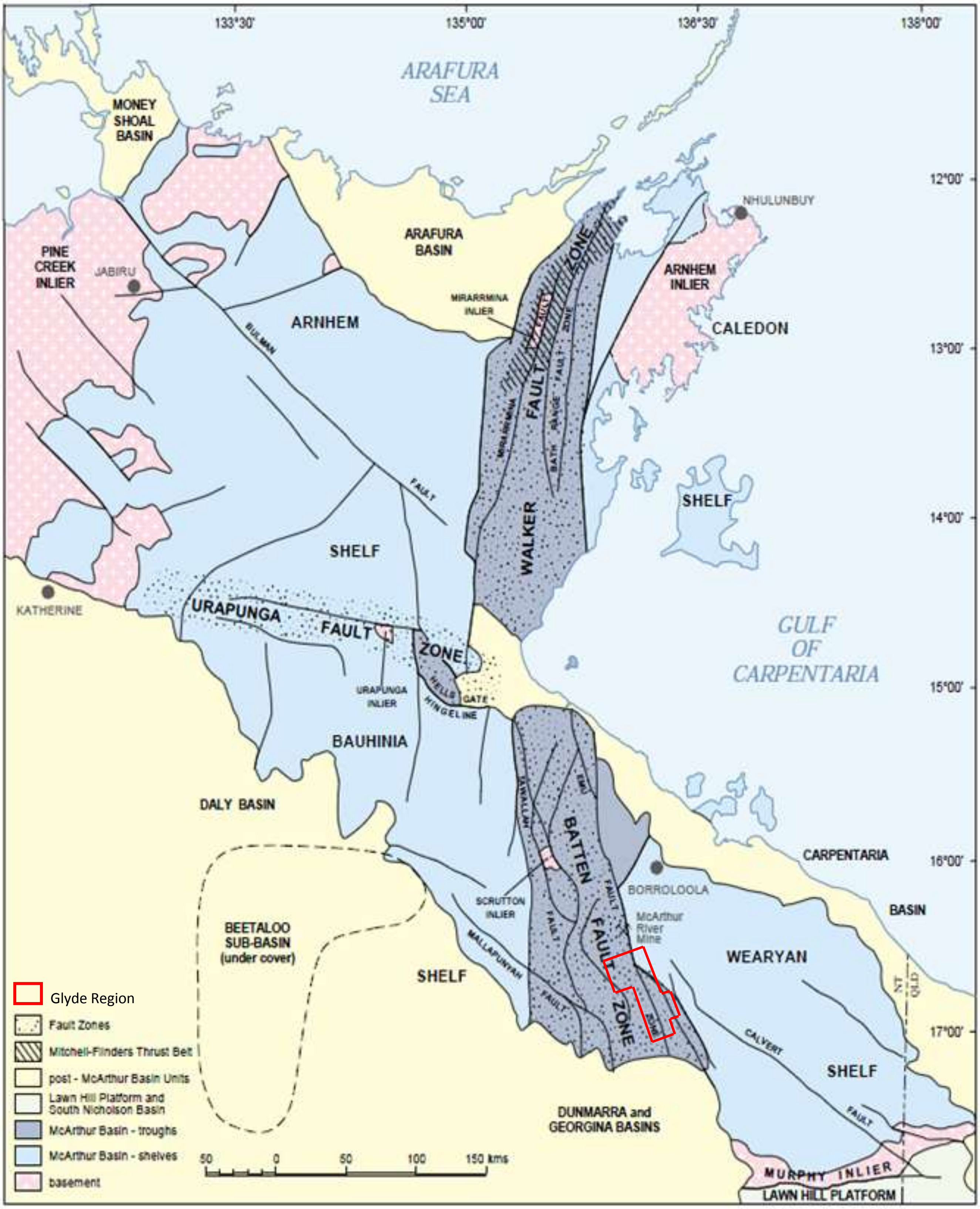

Figure 1 – Map showing regional structure and locality of the study area within the McArthur Basin.

2. Geological Background

2.1. Stratigraphy

2.1.1. Upper McArthur Group Stratigraphy

The McArthur Group ranges in age from approximately 1600 to 1700 Ma old (Page 1981). It is subdivided into the Umbolooga Subgroup and the Batten Subgroup (Figure 2.1.1).

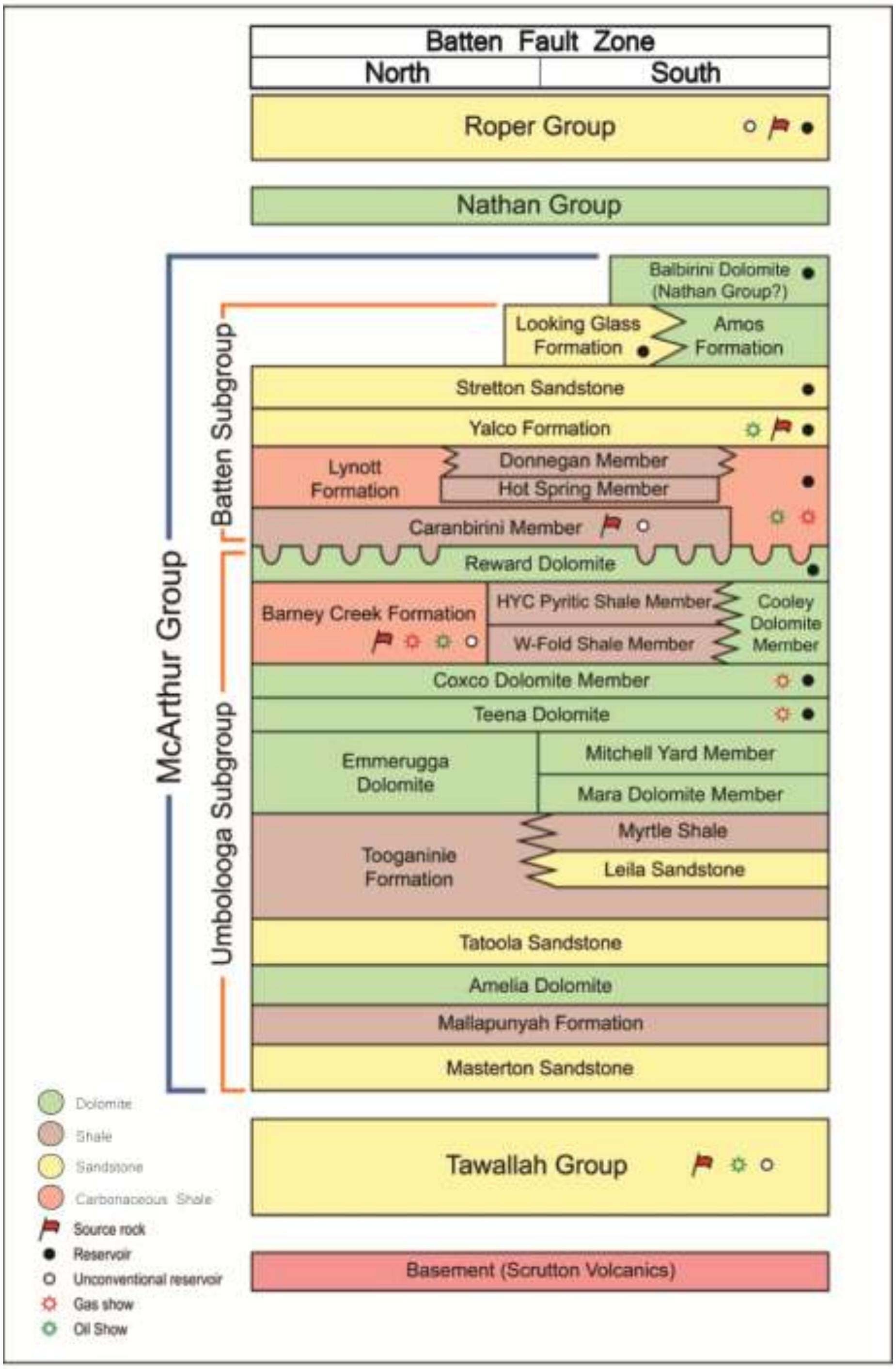

Figure 2.1.1 - Generalised McArthur Group Stratigraphy from north to south in the Batten Fault Zone (modified from Rawlings 1999).

McArthur Group stratigraphy intersected by wells in the Glyde region ranges from the Myrtle Shale to the Yalco Formation. In this region the McArthur Group is commonly overlain unconformably by the Bukulara Sandstone, which is Cambrian in age and overlies the Roper Group (Figure 2.1.1). Each of these formations will be briefly described in terms of mineralogy and structure, this review focusing mainly upon the Barney Creek Formation.

Myrtle Shale

The Myrtle Shale consists mainly of a red-brown siltstone and very fine-grained sandstone with infrequent, thin interbeds of coarse-grained sandstone, oolitic dolarenite, dololutite, and silty dololutite (Jackson et al. 1987). Brown et al. (1969) suggests that the siltstone is a subaerial deposit comprise primarily of wind-blown dust with the dolutlite interbeds deposited during incursion of seawater or within salt lakes formed through flooding.

Emerugga Dolomite (Mara Dolomite Member and Mitchell Yard Member)

In general, the Emerugga Dolomite consists of dolostone (with or without stromatolites), minor breccia, siltstone sandstone and infrequent potassium-rich mudstone (Jackson et al. 1987). Plumb and Brown (1973) divided this unit into two members; the Mara Dolomite Member and the Mitchell Yard Member. The major difference between the two members is that the Mitchell Yard Member is largely not silicified in contrast to the Mara Dolomite Member (Jackson et al. 1987). Brown et al. (1969) bases his depositional environment interpretation on modern analogues for stromatolitic environments at the time such as the marginal-marine hypersaline lagoons at Shark Bay, Western Australia. However, more recent studies suggest that stromatolites can occur in a variety of environments including groundwater lakes (Walter, 1976).

Teena Dolomite

The overlying Teena Dolomite is comprised of laminated and thinly bedded dololutite which is interbedded with intraclast conglomerates, dolarenite, dolomitic siltstone, sandstone and potassium-rich mudstone (Jackson et al. 1987). According to Davidson and Dashlooty (1993) gypsum casts suggest that the depositional environment is likely to be a shallow brine pool. In Contrast, Jackson et al. (1987) favoured a lacustrine setting for this formation. Figure 2.1.2 the probable

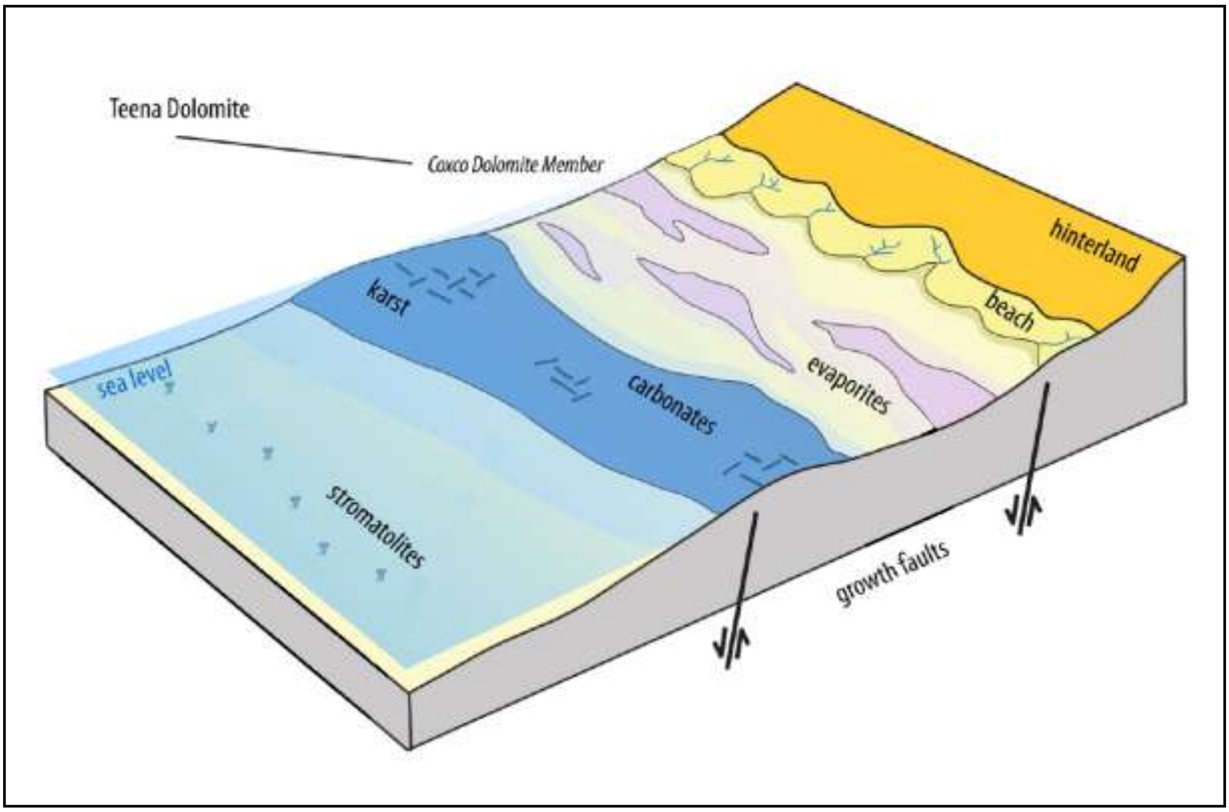

Figure 2.1.2 – Pictorial representation of the possible depositional setting for the Teena Dolomite, Coxco Dolomite and other similar formations within the Upper McArthur Group (Smith & Schmid, 2014).

Coxco Dolomite Member

The Coxco Dolomite is also largely dololutite, but tends to be more thickly bedded in comparison to the Teena (Plumb & Brown 1973). There are also thinner dololutite interbeds and frequent interbeds of pink potassium rich mudstones which have been identified as possible volcanic tuffs (Jackson et al. 1987). The depositional environment is believed to be very similar to that of the Teena Dolomite.

Barney Creek Formation (W-Fold Shale, HYC Pyritic Shale Member and Cooley Dolomite Member)

The Barney Creek Formation includes the W-Fold Shale, HYC Pyritic Shale Member and the Cooley Dolomite Member. In addition, the Cooley Dolomite Member interfingers with these members in the south of the Batten Fault Zone (Jackson et al. 1987). However, the bulk of the Barney Creek Formation (Undivided Barney Creek Formation) consists of uniform interbedded dolomitic siltstones, dolarenite and volcanic tuffs (Davidson & Dashlooty 1993). Logan and Williams (1984) describe a shallow water facies with dessication structures and a deep water facies with graded turbidite beds, flame structures, cross-beds, scours and load casts.

W-Fold Shale

The W-Fold Shale is the basal unit of the Barney Creek Formation and consists of green and red dolomitic, potassium-rich siltstone and shale as well as vitric tuffs and thin beds of pink, bituminous dolomite (Jackson et al. 1987; Davidson & Dashlooty 1993). Tuffs generally have a green colouration and become more abundant towards the top of the W-Fold Shale (Brown et al. 1969). Sedimentary structures include graded beds, scour structures, flame structures and ripple marks (Jackson et al. 1987). Thickness of this member is variable, ranging from zero in some parts of the basin to a maximum of about 150m (Davidson & Dashlooty 1993). A hyper saline brine pool / tidal flat depositional environment are proposed for this unit by Davidson and Dashlooty (1993).

HYC Pyritic Shale Member

The HYC Pyritic Shale Member overlies the W-Fold Shale and is a uniform dark-grey to black carbonaceous pyritic dololutite with scattered ovoid dolomite concretions and potassium rich mudstone interbeds ranging in thickness from zero to 50m within the Glyde Sub-basin (Davidson & Dashlooty 1993). Some of these mudstone interbeds contain glass shards and crystals which are indicative of a volcanic source (Jackson et al. 1987). The HYC Pyritic Shale Member is the most TOC rich member of the Barney Creek Formation and is thought to be the ‘sweet spot’ for unconventional petroleum. Logan and Williams (1984) suggest a lagoonal depositional setting with restricted circulation (Figure 2.1.3).

Cooley Dolomite Member

The Cooley Dolomite is a breccia consisting of clasts derived from the Emerugga and Teena Dolomites and inter-fingers with the other members of the Barney Creek Formation (Jackson et al. 1987). Hence, its mineralogical characteristics are similar to the sources from which it is derived (the Emerugga and Teena Dolomite). Deposition is thought to resemble a slump or alluvial fan (Figure 2.1.3)

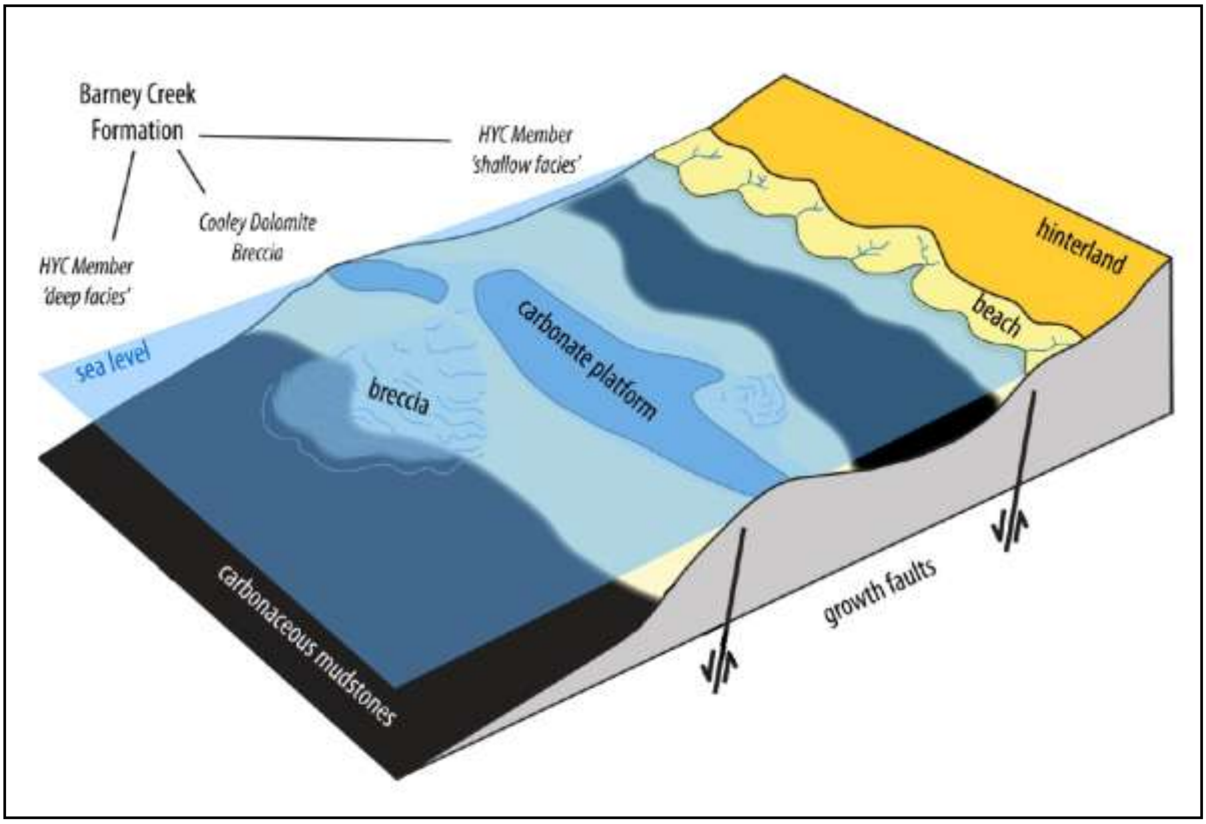

Figure 2.1.3 - Pictorial representation of the possible depositional setting for members of the Barney Creek Formation including the HYC Pyritic Shale and Cooley Dolomite (Smith & Schmid, 2014).

Reward Dolomite

There is a gradational transition from the Barney Creek Formation to the overlying Reward Dolomite which is an evaporitic dolomitic siltstone and pelletal, dolomitic sandstone with minor shale intervals and breccias (Pietsch et al. 1991). Brown et al. (1969) suggested several depositional environments due to variability in lithologies including shallow subtidal (stromatolites), lagoonal (gypsum), tidal channel (cross-bedded arenites) (Figure 5.1.4).

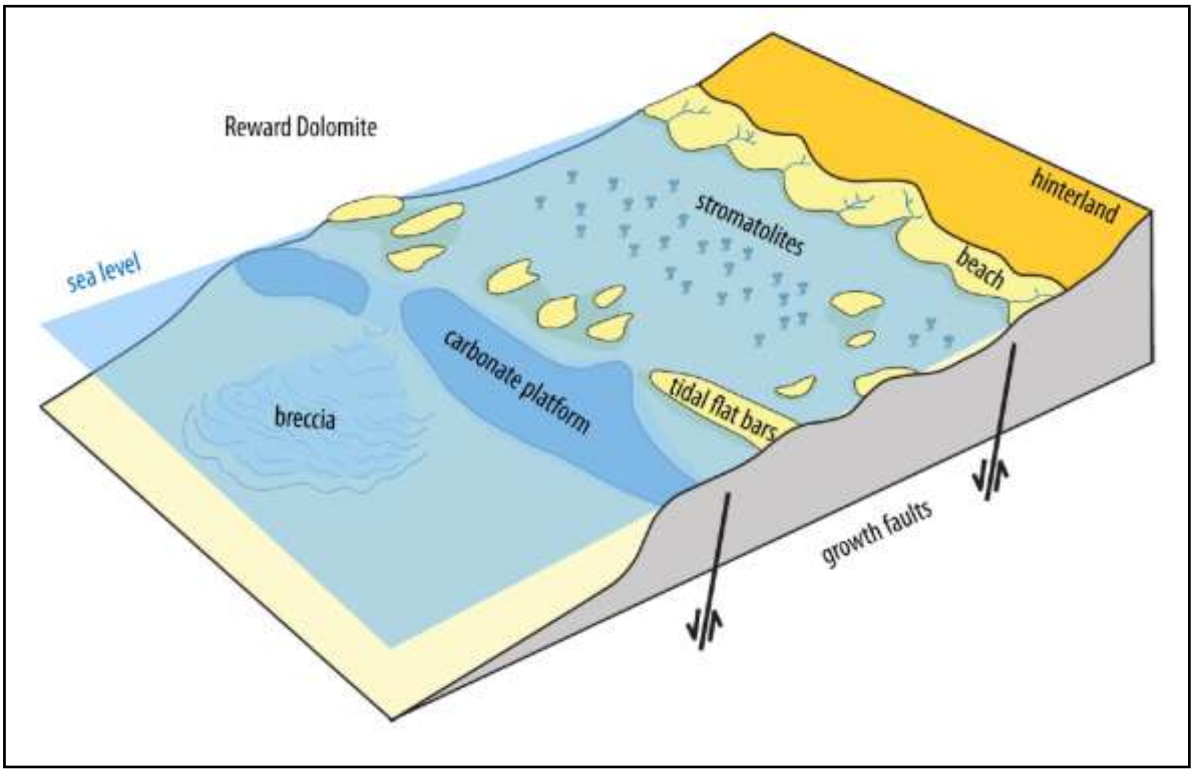

Figure 3.1.4 - Pictorial representation of the possible depositional setting for Reward Dolomite (Smith & Schmid, 2014)

Lynott Formation (Caranbirini Member, Hot Spring Member, Donnegan Member)

The Lynott Formation marks the change to the Batten Subgroup from the Umbolooga Subgroup. It can be subdivided into three members; the Caranbirini, Hot Spring and Donnegan which are described by Jackson et al. (1987). The Caranbirini Member is the basal unit of the Lynott Formation and is comprised of dolomitic siltstone, shale, and silty dololutite deposited in a lagoonal or lacustrine setting. The overlying Hot Spring Member consists of dolomitic siltstone, silty dololutite, dolarenite, stromatolitic dolostone and chert deposited in an intertidal environment. At the top of the Lynott Formation is the Donnegan Member, a purple-brown and green dolomitic, fine-grained sandstone and siltstone, with stromatolitic dolostone at the base believed to be representative of a sabkahh.

Yalco Formation

The Yalco Formation occurs in the middle of the Batten Subgroup and consists mainly of dolostone with stromatolites (Jackson et al. 1987). Muir et al. (1980b) likened the depositional environment of the Yalco Formation to ephemeral lakes within the modern day Coorong Lagoon, South Australia.

Bukulara Sandstone

The Bukulara Sandstone belongs to the Nathan Group and typically rests unconformably on the McArthur Group within the Glyde Sub-basin. It is Cambrian in age The Bukulara Sandstone consists of red thick to thin bedded fine to very coarse-grained feldspathic sandstone.

2.1.2. Summary

It is evident that the Upper McArthur Group consists of primarily shallow water facies and that most of the suggested depositional environments could be coexistent over a small area. The current train of thought is that structural complexities resulted in a series of carbonate platforms, hypersaline lagoons, intertidal zones and slightly deeper water zones as shown in Figure 2.1.5.

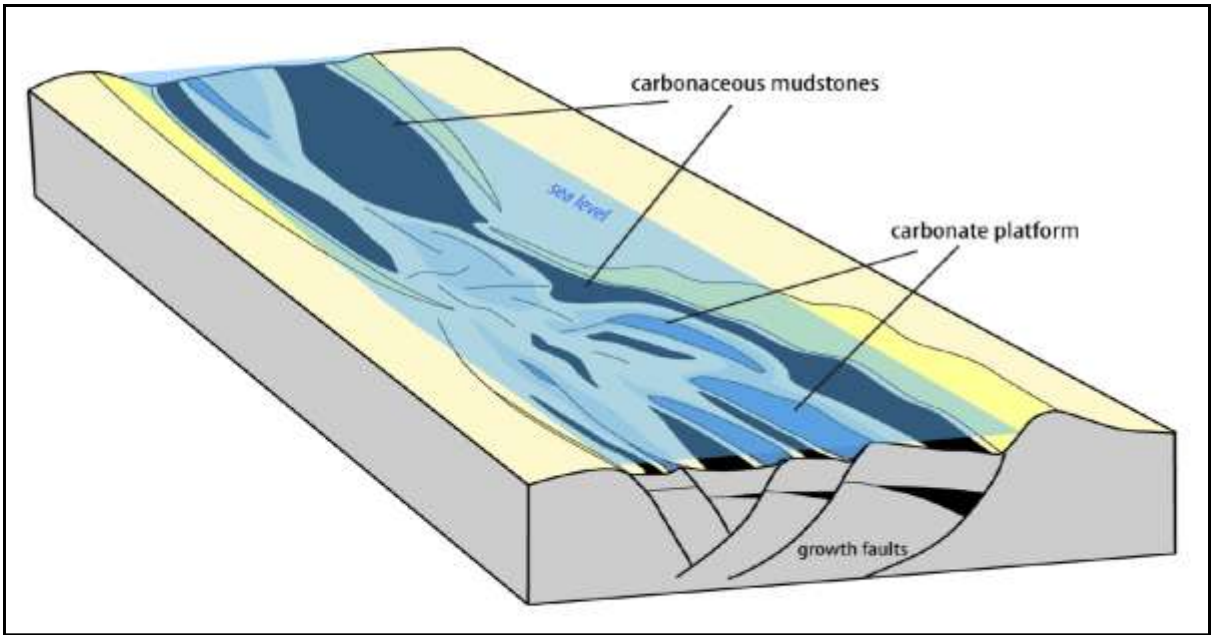

Figure 2.1.5 – Cartoon of a hypothetical depositional setting for the Glyde region (Smith & Schmid, 2014).

2.2. Structural Evolution of the Basin

2.2.1. Southern McArthur Basin

There are two current tectonic models for the formation of the McArthur basin; the ‘Plumb’ model and the ‘Etheridge and Wall’ model. Both models favour an extensional tectonic regime but differ in terms of orientation due to difficulty in determining primary structures which are overprinted by later structural inversion (Rawlings 1999). This project will focus on the more widely credited ‘Plumb’ model.

Several papers published by Plumb (1979, 1987), Plumb and Wellman (1987) and Plumb et al. (1980, 1990) present the evolution of the McArthur Basin using a framework of troughs, shelves and fault zones (Figure 1). This model suggests that east-west crustal extension over 200Ma was responsible for intermittent strike-slip faulting, block rotation and syn-sedimentary faulting which resulted in the development of the Batten Trough / Fault Zone (Figure 1). Tawallah Group (Figure 2.1.1) deposition is believed to be controlled by a series of linked north – south striking extensional faults, including the Emu Fault (Figure 1). These faults represent the preliminary stages of the Batten Fault Zone which is the primary depositional site during McArthur Group time. Subsequent deposition of the McArthur Group was controlled by rifting of the Batten Trough through oblique, north-west to north extension (Plumb 1994; Davidson & Dashlooty 1993). Faults trending in a north-northwest to north-northeast direction were reactivated in a right lateral sense while north-west trending faults were reactivated in a left lateral sense. This resulted in the formation of large pull-apart basins, including the Glyde Sub-basin. Right lateral motion along the Emu Fault led to growth faulting which resulted in stratigraphic thickening adjacent to the fault, most notable in the Barney Creek Formation (Rawlings 1999).

2.2.2. Glyde Sub-basin

The deep fault-bounded nature and fault orientations within the Glyde sub-basin are typical of a right-lateral pull apart basin (Davidson & Dashlooty 1993). Basin formation is suggested to have occurred in three main phases according to Davidson and Dashlooty (1993).

(Phase 1) Initiation of sub-basin development commenced at the end of Coxco Dolomite Member deposition. During this time a segment of the Emu Fault deviated from the regional slip direction. The result was two side-stepping, en echelon fault strands which eventually bound the developing pull apart basin. At this stage, some of the major antithetic strike-slip faults begin to develop including the Wilkinson Fault (Figure 2.2.2a).

(Phase 2) Continued right lateral movement results in the formation of second generation antithetic strike-slip and normal faults in addition to some synthetic faults which divide the basin into several fault bounded blocks. Subsidence is at a maximum towards the end of W-Fold shale deposition. Sinuosity of the Emu Fault trace is likely to have been caused by local transpressive forces which resulted in thrusting / reverse faulting in this section (Figure 2.2.2b).

(Phase 3) Subsequent locking of this transpressive zone on the Emu Fault results in straightening of Fault trace and formation of Block 7 (Figure 2.2.2c). Thrusting / reverse faulting and uplift occurs immediately north of this location. At this time, the major elements of the basin have been formed which coincides with the beginning of undifferentiated Barney Creek Formation deposition. The generation of fault strands sub-parallel to the regional trend of the Emu Fault Zone marked the end of basin deepening.

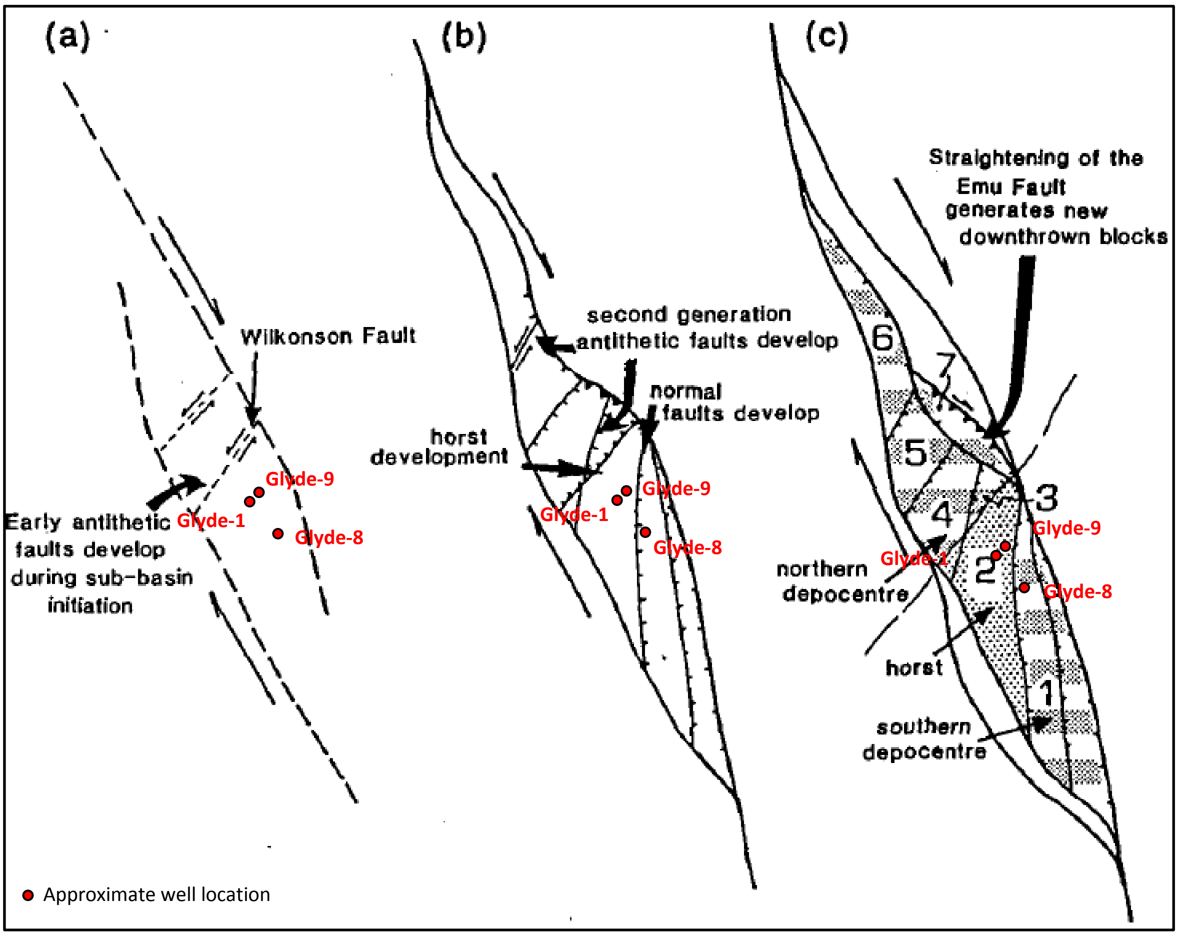

Figure 2.2.2. - Generalised McArthur Group Stratigraphy from north to south in the Batten Fault Zone (Modified from Rawlings 1999).

The fact that the Barney Creek Formation is typically overlain by the Bukulara Sandstone, as previously mentioned, indicates post Barney Creek uplift and significant erosion prior to deposition of the Nathan Group. There is also indication of post Roper Group compression indicated by joint pattern development along the Emu Fault Zone in the Bukulara Sandstone (Harding 1974). This also suggests that much of the deformation which has occurred after basin formation has involved inversion of older structures.

The 3 wells located in the Glyde Sub-basin will be used to evaluate the difference in sediment packages deposited within the horst (Block 2) in comparison to the downthrown Block 1.

2.3. Present Day Basin Structure

At a regional scale the Glyde region can be broken into six structural domains (Figure 2.3); the Borroloola Block, Emu Block, Glyde Sub-basin, 'Pop up' structure, Raised Fault block and the NW-SE Fault Zone.

The major structure within the area is the Emu Fault Zone which separates the Borroloola Block from the Emu Block. It is widely recognised that the Emu Fault was a major structural feature in the central-southern part of the McArthur Basin and was a major control on depositional geometry (e.g. Rawlings et al. 2004 and Korsch et al. 2005). The two anastomosing branches of the Emu Fault Zone that bound the Glyde Sub-basin form raised fault blocks or horsts with the basin itself being the graben. The pop up structure is the result of transpression along the Emu Fault Zone which is exemplified by reverse, transpressional and strike-slip faults aswell as abundant anticlines and synclines in the northern part of the survey area (Figure 2.3). Post Roper inversion is responsible for the NW-SE trending Fault zone as well as overprinting of many of the older structures within the region (Harding 1974).

It is expected that depositional histories within each of these structural domains is highly variable. This will be assessed using well data from 6 wells from three different structural domains; the Glyde Sub-basin, the bounding raised fault blocks of the Emu Fault Zone and the Emu Block (Batten Fault Zone).

*Please note well BJ2 lies outside of the structurally interpreted area.

**For location of survey data area refer to Figure 1.

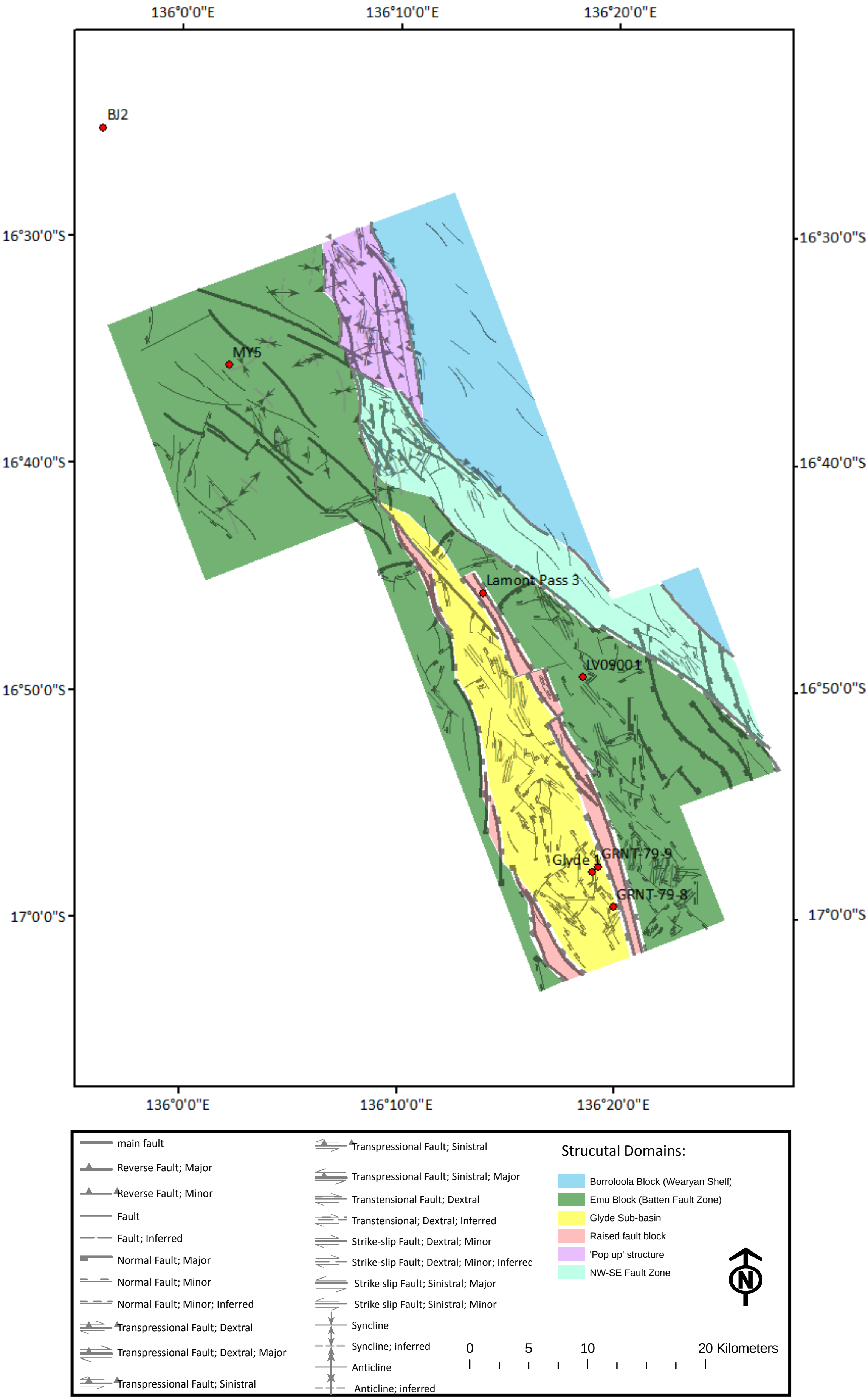

Figure 2.3 - Structural interpretation of Glyde region from FALCON gravity survey (Kovac 2013).

3. Stratigraphic Methods

3.1 Wells

As previously mentioned, a combination of petroleum and mineral hole data will be used for the purposes of the project. The table below summarises each well and the data used for interpretation.

Well	Well Type	Data Available
GR-8 (GRNT-79-8)	Mineral exploration	HyLogs, core photos, gamma plots / spectral gamma plots and well completion reports.
Glyde-1	Petroleum	Wireline logs (gamma, sonic, density, resistivity), XRF and TOC data.
Glyde 9 (GRNT-79-9)	Mineral exploration	HyLogs, core photos and well completion reports.
LV-9 (LV09001 or Leviathan 9)	Mineral exploration	HyLogs, core photos, gamma plots / spectral gamma plots and well completion reports.
Lamont Pass-3	Petroleum	Wireline logs (gamma, sonic, resistivity) and XRF data.
MY 5 (Myrtle 5)	Mineral exploration	HyLogs, core photos, gamma plots / spectral gamma plots and well completion reports.
BJ2 (Berjaya 2)	Mineral exploration	HyLogs, core photos, gamma plots / spectral gamma plots and well completion reports.

3.2 Mineral Well Interpretation

3.2.1 HyLog Data

HyLogging is a method of reflectance spectroscopy developed by the Commonwealth Scientific and Industrial Research Organisation (CSIRO) to sample drill core, chips or powder. It involves exposing the sample to an energy source and measuring the reflectance from the same at various wavelengths using a spectrometer. Each minerals unique reflectance spectra allows for identification of specific mineral or mineral groups.

HyLog data provided for each well was obtained from HyLogging drill core and viewed using TSG Viewer. The two main HyLog tracks used for interpretation are the primary short wave infra red spectrum and the primary thermal infra-red spectrum. The primary SWIR log allows for visualisation of the abundance of key minerals within the section. This permitted the identification of changes in specific minerals that could be specific to a certain interval within a formation. A key note with this track is that 'aspectral' mineralogy refers to a reading which is so low because the sample absorbs the majority of the energy, which usually indicates a dull, dark core. The primary TIR log displays the distribution of key mineral groups over the interval. This provided an overview of how the lithology was changing within a single formation. For example, it can indicate whether a formation is becoming more silica rich (i.e. sandier). With this track it is important to note that 'invalid' refers to a signal which is unrecognisable by the analyser. The responses in these tracks are measured in counts which refer to the number of times a particular signal is measured for a set number of samples over a given interval or 'bin'. The bin size was set individually for each well to maximize the resolution without distorting the tracks.

In addition to these tracks an albedo and core photo plot were used for interpretation. The albedo track is basically a graphical representation of the cores average reflectivity within each bin. Lighter sediment colouration and hence lighter minerals would register a higher albedo and vice versa. Next to this is, a track containing a photo of the core tray that corresponds with each bin to give an idea of core colouration. This way there are both quantitative and qualitative representations of core colour.

3.2.2 Gamma Logs

In addition to this, some of the mineral wells had accompanying gamma log data which was collected using a hand-held logger from the core. The data set consisted of a gamma reading in counts per second (cps) taken every 0.5m along the drill core which was plotted in excel. The gamma log responds to changes in gamma radiation from decay of uranium, potassium and thorium. Clay rich facies tend to be rich potassium and have high gamma readings while sand rich facies are the opposite. Carbonates also tend to have low gamma counts and hence the gamma log can be used to visualize changes in lithology.

3.2.3 Facies Determination

Formation tops were cross-checked and replaced based on obvious mineralogical changes as a preliminary step in dividing each HyLog into a set of manageable geochemical facies. Using the previously described tracks in combination each formation further divided into a set of facies. A significant change in any one of the four tracks would warrant the definition of a new facies.

The purpose of this is to allow for the evaluation of the thickness and distribution of specific portions of a formation as opposed to the entire formation itself to gain a better understanding of depositional patterns. This is helpful because the zones of interest do not encompass the entire Barney Creek Formation and it is important to identify what portion of the formation is a desirable target and how this is distributed across the Glyde region. In addition, facies determination allows for review of depositional environments for each formation which may correspond with certain facies defining characteristics.

3.3 Petroleum Well Interpretation

The same idea is employed for the petroleum well interpretation with the only difference being the data set. Formations are divided into units rather than facies purely for easier differentiation of the results during the discussion. Instead of using HyLog and core data, a composite log of wireline, XRF and TOC data will form the basis of the interpretation.

3.3.1 Wireline Logs

The available wireline logs include gamma, sonic, density and resistivity.

The gamma log data for the petroleum wells is generated using a wireline gamma tool which measures the gamma count in the borehole. These measurements are given in gAPI which is a unit derived by the American Petroleum Institute and roughly equates to 1cps.

The sonic log measures a formations interval travel time or ability to transmit seismic waves which is given in microseconds per foot (µs/ft). This value is variable with lithology and can provide an idea of effective porosity. A more porous formation will have a lower sonic reading then a non-porous, compact formation.

Density, measured in grams per cubic centimetre (g/cm^3) also gives an indication of compactness as well as density of constituent minerals.

Resistivity data is collected using electrodes with varied spacing to investigate different borehole wall depths to avoid effects of drilling fluids. The logs used include the shallow laterlog (DSLL), micro pad resistivity (MRRS) and the deep later log (DDLL). These logs measure a formations ability to transmit an electrical current given in ohm metres (ohm.m). A high resistivity can indicate a high metal content or saline formation water while a low resistivity may indicate low porosity or hydrocarbon content for example.

3.3.2 XRF Data

XRF stands for X-Ray Fluorescence and is a method of spectroscopy, similar to HyLogging. XRF data gives a graphical representation of concentrations of various elements or compounds over the well interval given a s a percentage of the total sample volume or in parts per million (ppm). Selected XRF data was displayed based on the variability of the specific element or compound throughout the section. For example, the plots which seemed to display a constant concentration throughout the section were omitted as they were not useful for dividing the formations into individual units.

3.3.3 TOC Data

Total Organic Carbon (TOC) data for Glyde-1 is obtained using a LECO Carbon Analyser which measures the amount of TOC after pyrolysis of a dried and leeched sample. Samples for Glyde-1 are representative of 10m intervals. Each value is then plotted at the median depth for which it represents.

TOC data is probably the most critical part of the petroleum well interpretation as it permits identification of the TOC rich zones which may be potential petroleum targets.

3.4 Correlation

Correlation between all wells is difficult due to the wide variation in formations identified and wouldn't offer anything beneficial. However it is important to understand the relationship between petroleum and mineral well data so that specific data such as TOC can be extrapolated across the study area. The most appropriate method of doing so is to correlate a petroleum well with a mineral well. This will be completed using the Glyde-1 and Glyde-9 interpretations as these wells are situated in close proximity within the same structural domain which will make for the most accurate correlation possible.

4. HyLog Interpretation

4.1 Facies Description

Facies will be described individually by formation in chronological order from oldest to youngest. Glyde-8 intersects the Bukulara Sandstone and the Barney Creek Formation (including the W-Fold Shale). The Bukulara Sandstone also overlies the Barney Creek Formation in Glyde-9 which also intersects the Cooley Dolomite and Coxco Dolomite. Myrtle-5 unexpectedly intersects the Surprise Creek Formation in addition to the Reward Dolomite, Barney Creek Formation (including the HYC Pyritic Shale and W-Fold Shale) and the Teena Dolomite. The undivided Lynott Formation, Reward Dolomite, Barney Creek Formation and Teena Dolomite are present in the Berjaya 2 interval. Leviathan 9 intersects the Mitchell Yard Member, Teena Dolomite, Barney Creek Formation, Reward Dolomite, Caranbirini Member, Hot Spring Member, Yalco Formation, Bukulara Sandstone and the oldest formation of the mineral wells; the Mara Dolomite.

Mara Dolomite (MD)

MD Facies 1

The Mara dolomite, observed in Leviathan 9 (Figure 4.1.1) consists of only one facies as it is very uniform in terms of mineralogy, albedo and core colour. The SWIR spectrum is limited to ankerite and dolomite with dolomite being much more prevalent. The TIR spectrum shows only silica and carbonates. Surprisingly, the albedo is in the medium range and the core colour is light – dark grey.

Mitchell Yard Member (MY)

MY Facies 1

The Mitchell Yard Member is highlighted by and abrupt change in the TIR and SWIR spectrum as well as a sharp decrease in albedo between Teena and Mara Dolomites in Leviathan 9 (Figure 4.1.1). The

SWIR shows very minor phengite, ankerite and dolomite with aspectral mineralogy predominating. The TIR spectrum shows potassium feldspar which makes the facies very distinctive in this track.

Teena Dolomite (TD)

TD Facies 1

The facies, observed in Myrtle 5 (Figure 4.1.3) is very uniform in terms of mineralogy. This facies is identical to MD Facies 1, having a SWIR spectrum limited to ankerite and dolomite and a TIR spectrum that shows only silica and carbonates. Surprisingly, the albedo is in the medium range and the core colour is light – dark grey.

TD Facies 2

In Myrtle 5 (Figure 4.1.2) the SWIR spectrum shows only dolomite whilst the TIR spectrum shows potassium feldspar and carbonates for the Teena Dolomite. Albedo is higher in comparison to TD facies 1 as the core colour is a significantly lighter off white. Gamma data is available and shows an average of about 400cps for this facies.

TD Facies 3

This facies is observed in Berjaya 2 (Figure 4.1.3) and is identical to TD facies 1 with the only exception being the absence of silica in the TIR spectrum.

Coxco Dolomite (CX)

CX Facies 1

Much like the Cooley Dolomite, the Coxco Dolomite, which is also observed in Glyde-9 (Figure 4.1.4) has an SWIR spectrum consisting of ankerite and dolomite. The TIR spectrum shows only carbonates and the albedo is very high which corresponds with the almost white core colouration for this interval.

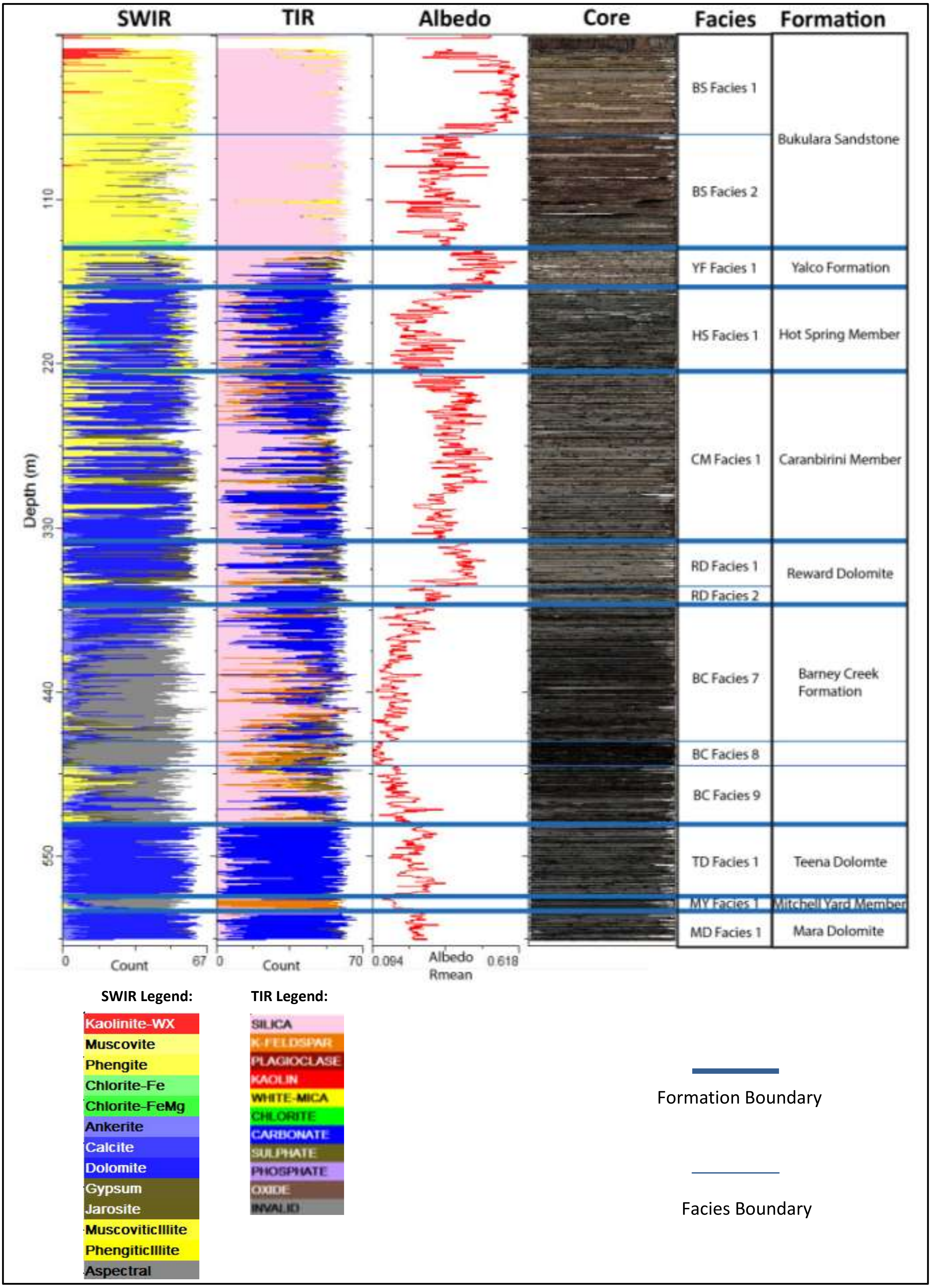

Figure 4.1.1 – Leviathan 9 HyLog, Core Photo Facies Interpretation

W-Fold Shale (WF)

WF Facies 1

The W-Fold Shale is easily distinguishable from the rest of the Barney Creek Formation in Glyde-8 (Figure 4.1.5) due to the abundance of carbonates in both the short wave and thermal infra-red spectra. A higher albedo is also distinctive which reflects the light grey core colour.

WF Facies 2

Basal facies dominated by dolomite in the SWIR spectrum with minor phengite it is indistinguishable from TD facies 2, which underlies it in Myrtle 5 (Figure 4.1.2).

HYC Pyritic Shale (HYC)

HYC *Facies 1*

The SWIR spectrum of the HYC pyritic shale shows predominately aspectral mineralogy with minor gypsum while the TIR spectrum cannot be differentiated from BC Facies 3. The albedo is extremely low and the core colour is almost black. The gamma log shows an average of approximately 400cps for this facies.

Cooley Dolomite (CD)

CD Facies 1

The Cooley Dolomite is relatively uniform in terms of its SWIR spectrum which includes ankerite and dolomite. Likewise, the TIR spectrum shows only silica and carbonates. Both the mineralogical change and the sharp increase in albedo make the Cooley Dolomite easily identifiable in Glyde-9 (4.1.4).

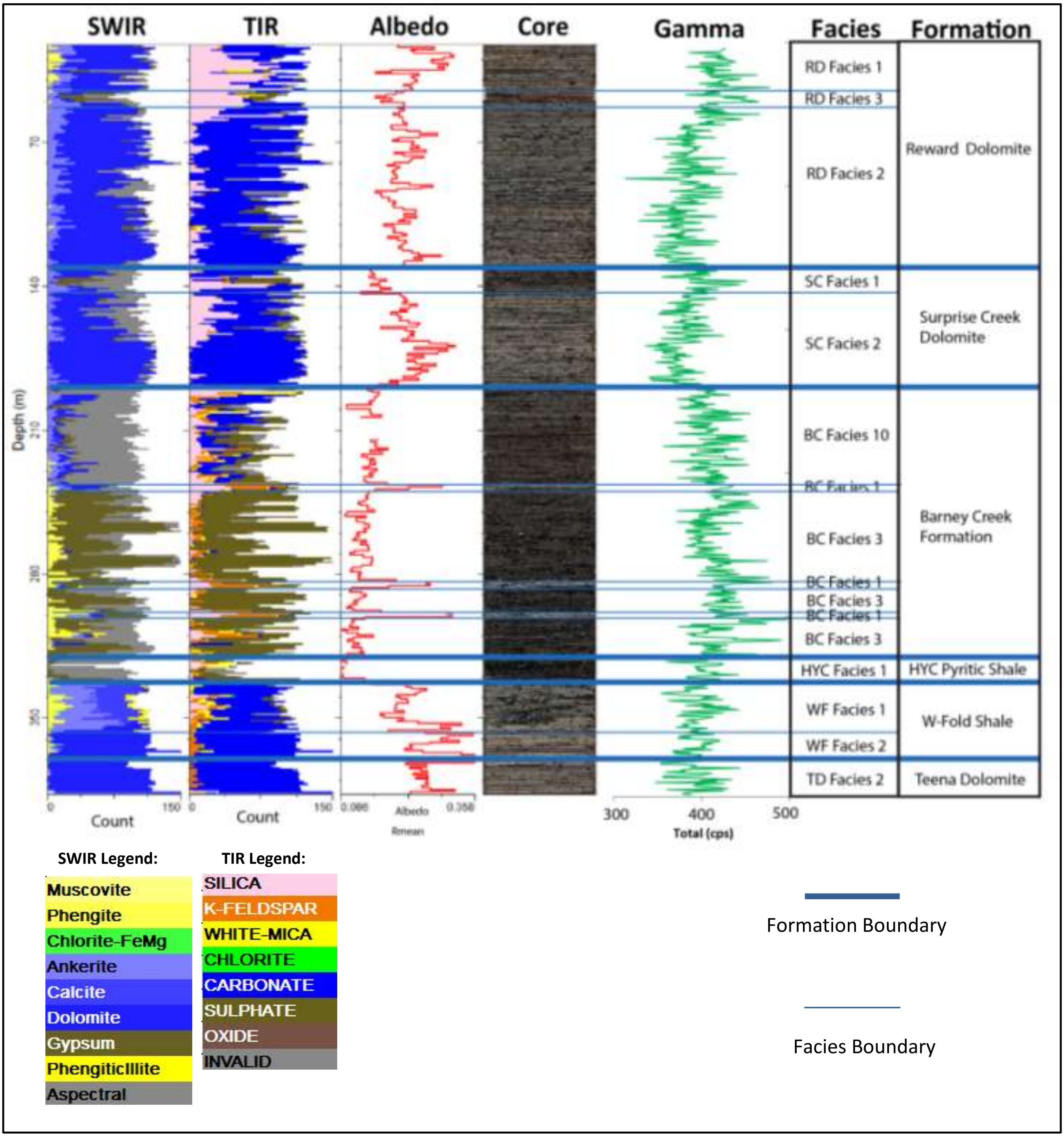

Figure 4.1.2 – Myrtle 5 HyLog, Core Photo and Gamma Facies Interpretation

Barney Creek Formation (BC)

BC Facies 1

Probably the most prominent facies within the Barney Creek Formation due to its sharp albedo peak and very light core colour. The presence of phengitic illite in the thermal infra-red spectrum separates it from other Barney Creek facies. The shortwave infra-red spectrum shows white micas, feldspars and silica. Gamma is not outstanding from the other facies in Myrtle 5 (Figure 4.1.3) and Glyde-8 or 9 (Figure 4.1.5 and 4.1.4 respectively) but core colour is a very light grey.

BC Facies 2

Characterised by muscovite, phengite and aspectral mineralogy in the short wave infra-red spectrum. Thermal infra-red is dominated by carbonates, silica with smectite dispersed throughout and typified by the presence of invalid and a lack of sulphates. The gamma count for this facies is much higher than the surrounding rocks in Glyde-8 (Figure 4.1.4). Other than these differences, it is identical to the majority of the Barney Creek Formation in terms of its short wave infra-red spectrum, albedo and core colour.

BC Facies 3

The third facies identified within the Barney Creek Formation is almost identical to Facies 2 in terms of geochemistry, with the addition of sulphates in the thermal infra-red spectrum and a decrease in distribution of invalid mineralogy. The boundary between the two facies is marked by a significant drop in the gamma count. Core colour is light to dark grey and albedo and gamma fluctuate in the lower range indicating small scale variations.

BC Facies 4

Identical to facies 3 aside from an increase in sulphates detected in the short wave infra-red spectrum and a distinct red-brown core colouration.

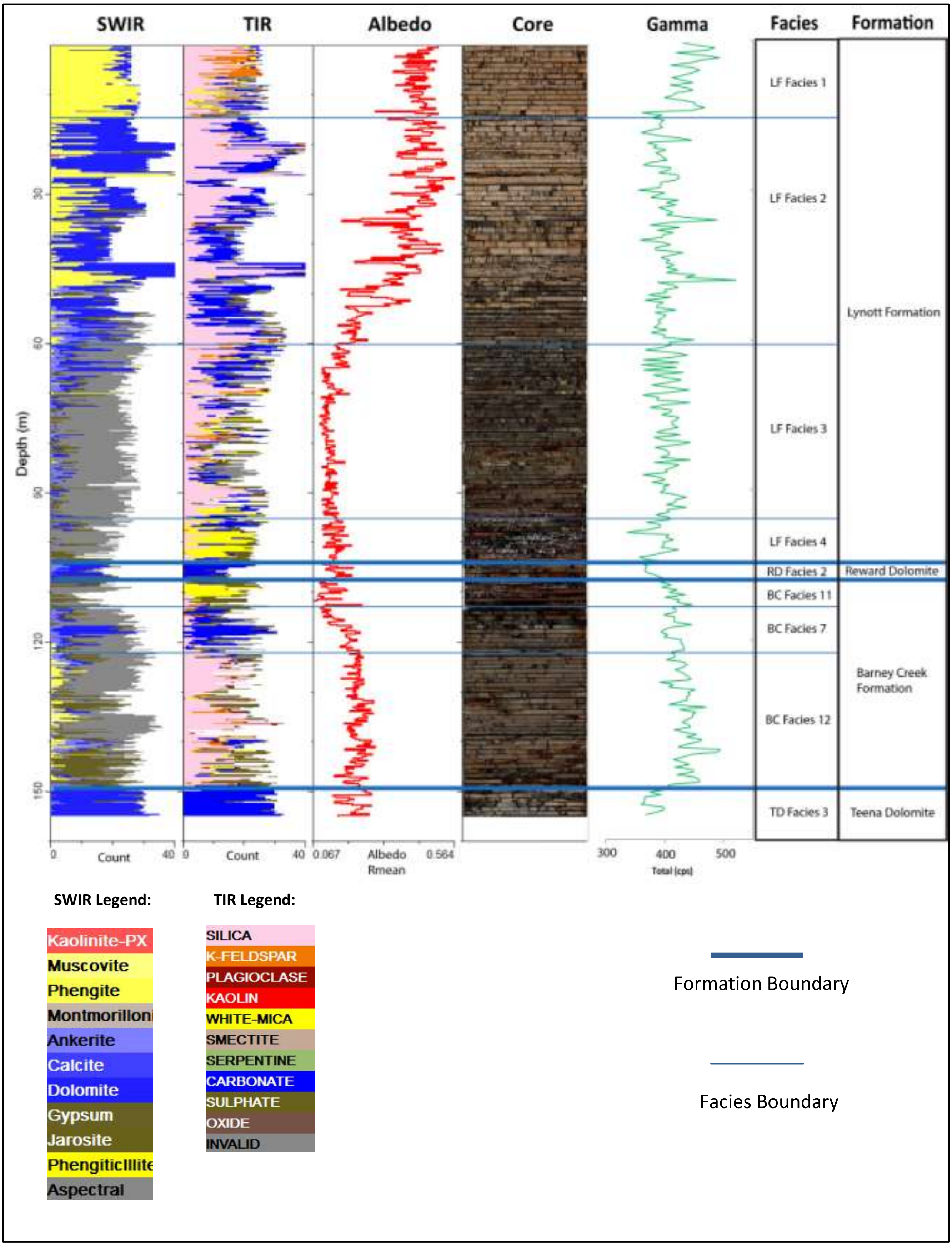

Figure 4.1.5 – Berjaya 2 HyLog, Core Photo and Gamma Facies Interpretation

BC Facies 5

Facies 5 is similar to facies 1 in the thermal infra-red spectrum as well as the distinctive, sharp albedo peaks. However, in the short wave infra-red spectrum in addition to silica there is ankerite and dolomite. Core colour is not dissimilar from the surrounding rock.

BC Facies 6

The only attribute that sets this facies apart from BC Facies 3 is a notable drop in albedo to almost zero and a dark grey to almost black core colouration.

BC Facies 7

Dominated by aspectral mineralogy in the SWIR spectrum with ankerite, dolomite and minor phengite. Silica, carbonate and potassium feldspar make up the TIR spectrum. Albedo fluctuates but is low on average and core colour is dark grey.

BC Facies 8

Aspectral mineralogy accounts for almost the entire SWIR spectrum with very minor gypsum and ankerite. The TIR spectrum is not dissimilar from Facies 7 aside from a lack of carbonates and an abundance of potassium feldspar. Core colour is essentially black with a very low albedo reading.

BC Facies 9

Facies 9 shows similarities with facies 7 with the most notable difference being an abundance of phengite in the SWIR spectrum.

BC Facies 10

This facies is unique to Myrtle 5 (Figure 4.1.4) and is the uppermost constituent of the Barney Creek Formation in this well. Gamma, core colour and albedo are the same as BC Facies 3; however aspectral mineralogy is more dominant in the SWIR spectrum with ankerite and dolomite with minor gypsum. The TIR spectrum includes silica, potassium feldspar, white-mica, carbonate, sulphate and invalid mineralogy.

BC Facies 11

This facies which is unique to Berjaya 2 (Figure 4.1.3) is mineralogical simple with only gypsum and aspectral mineralogy comprising the SWIR spectrum and white-mica dominating the TIR spectrum. Albedo is low and the core colour appears black with a white mottling which seems unusual and has been suggested to indicate alteration of the core.

BC Facies 12

Silica, feldspars and sulphates comprise the TIR spectrum with silica being the most abundant by far. Aspectral mineralogy is the major component of the SWIR spectrum with gypsum, jarosite and muscovite and minor ankerite and dolomite. Gamma and albedo are slightly higher than the other BC Facies in Berjaya 2 (Figure 4.1.3) as the core colour is light grey.

Surprise Creek Formation (SC)

SC Facies 1

The SWIR spectrum for this facies consists of ankerite, dolomite, gypsum and aspectral mineralogy. Silica, carbonate, sulphate, invalid mineralogy and very minor potassium feldspar make up the TIR spectrum. The gamma plot shows an average reading slightly above 400cps and the albedo is low which corresponds with the dark grey core colour.

SC Facies 2

This facies is separated from SC facies 1 due to a change in core colour from dark grey to light grey which is also indicated by a higher albedo for this facies.

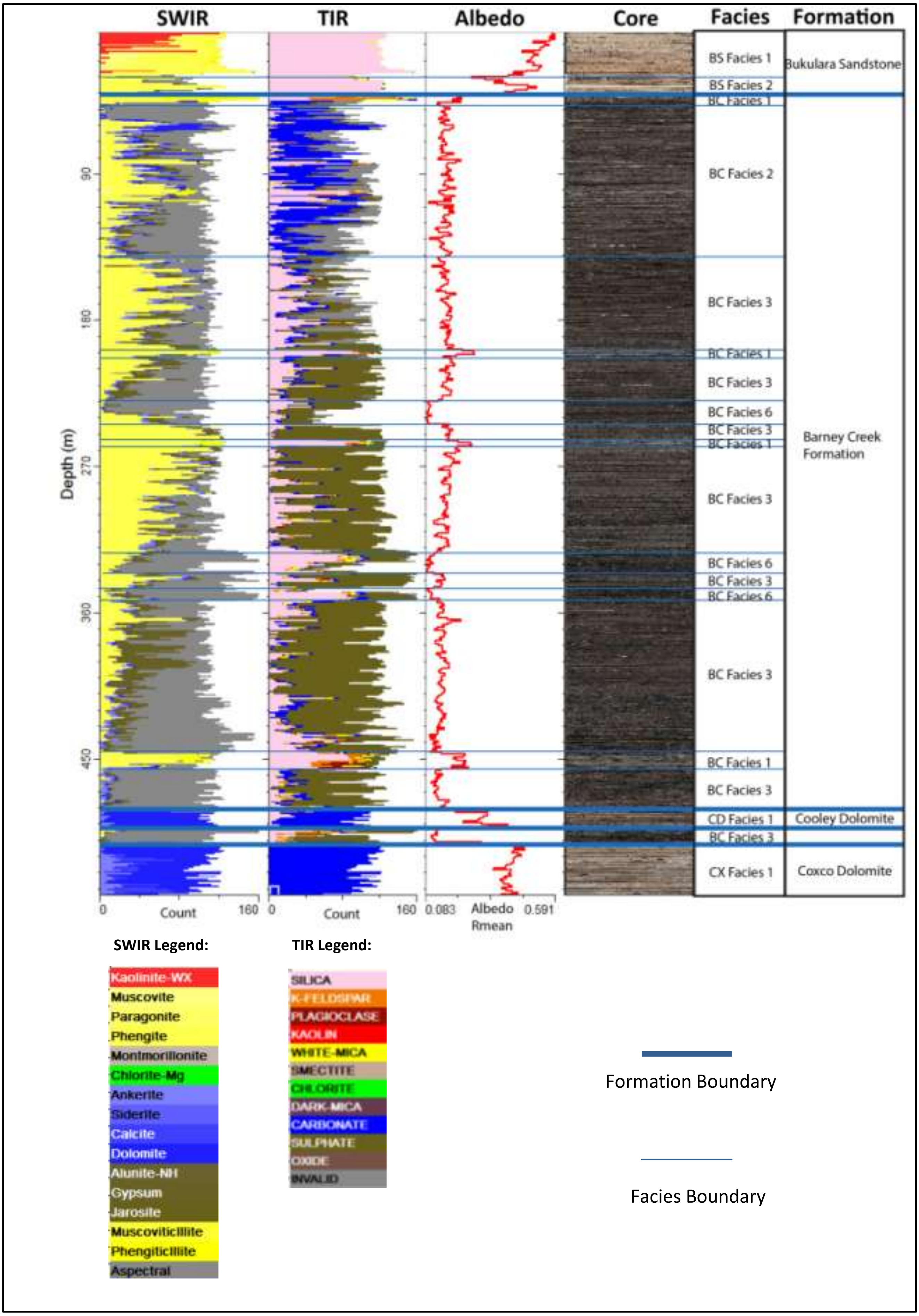

Figure 4.1.4 - Glyde-9 HyLog and Core Photo Facies Interpretation

Reward Dolomite (RD)

RD Facies 1

The SWIR spectrum for RD facies 1 is comprised of dolomite and phengite with minor ankerite and gypsum. Silica and carbonates comprise the TIR spectrum. There is a reasonably noticeable jump in albedo and lighter core colouration in comparison to the overlying Caranbirini Member.

RD Facies 2

Facies 2 is more uniform, consisting almost solely of Dolomite with minor ankerite and gypsum. Silica and carbonates comprise the TIR spectrum. Albedo and core colour are identical to RD facies 1.

RD Facies 3

The third Reward Dolomite facies identified in this well is seperated from the other two by the presence of gypsum in the SWIR and hence sulphates in the TIR spectrum. In addition to this, there is a drop in albedo and a distinctive brown-red core colour for this facies.

Hot Spring Member (HS)

HS Facies 1

The Hot Spring Member in Berjaya 2 (Figure 4.1.3) has a similar SWIR and TIR spectrum as the Yalco Formation besides the addition of chlorite. There is a clear drop in albedo as the core colour changes from light grey to dark grey.

Caranbirini Member (CM)

CM Facies 1

The only change from the Hot Spring Member facies is a slight change in core colour to the lighter grey along with an increase in albedo (Figure 4.1.3). Without being provided formation tops it would be very difficult to isolate this as a separate formation.

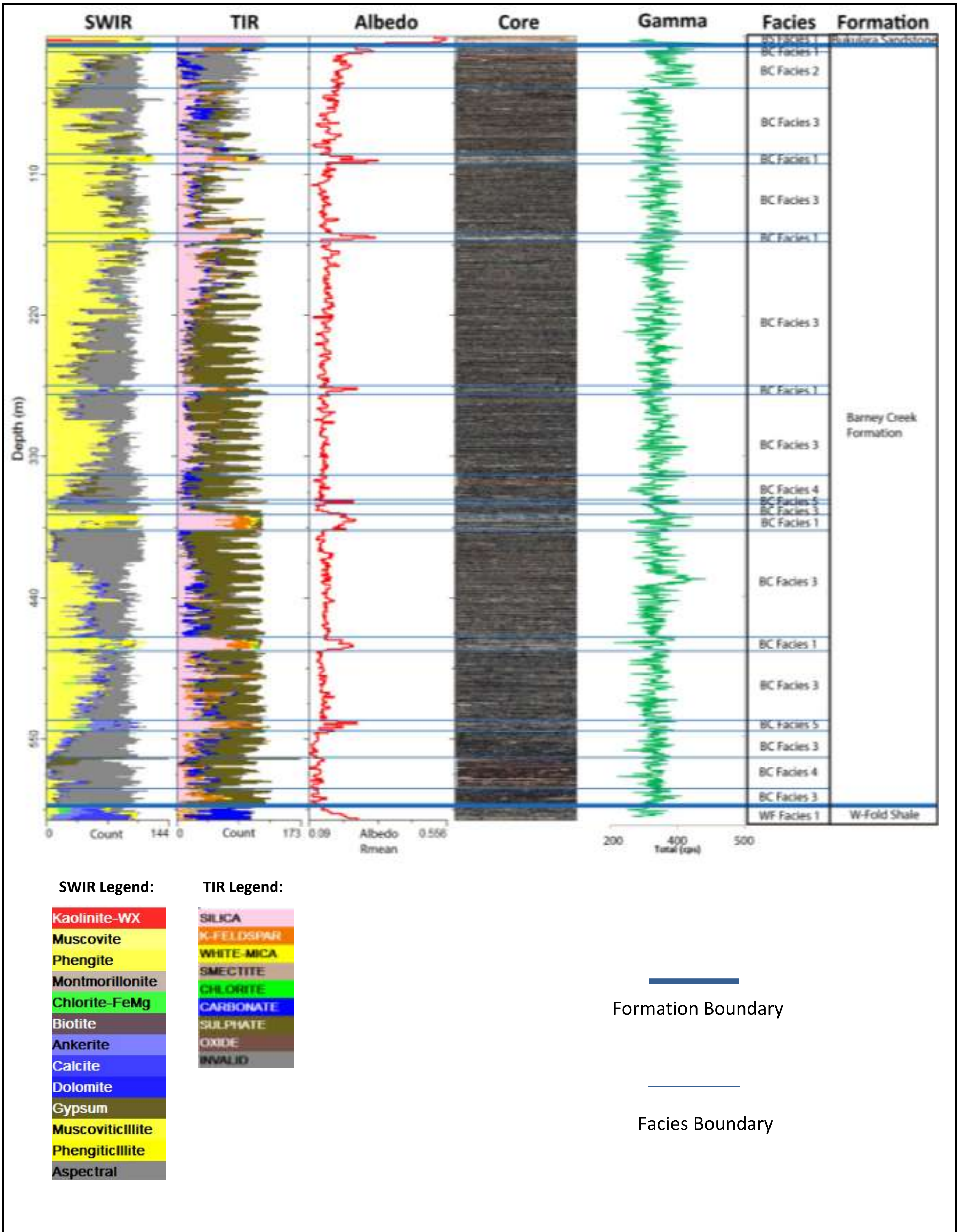

Figure 4.1.5 – Glyde-8 Hylog, Core Photo and Gamma Facies Interpretation

Lynott Formation (LF)

LF Facies 1

Characterised by muscovite and kaolinite in the short wave infra-red spectrum and only silica in the thermal infra-red spectrum. There is a very high albedo for this facies which reflects the almost white core colouration. Gamma count is also very high in comparison to the rest of the well.

LF Facies 2

Is marked by a significant decrease in the potassium feldspar count in the TIR sepctrum along with an increase in dolomite abundance shown in the SWIR sepctrum. Core colour and albedo remain the same as LF Facies 1 although there is a drop in gamma.

LF Facies 3

Separated due to the lack of phengite seen in the overlying facies and the appearance of aspectral mineralogy which corresponds with a large drop in albedo and a much darker core colouration. Gamma is consistent with LF Facies 2.

LF Facies 4

Identical to BC Facies 11 which is further evidence that the core has under some sort of alteration.

Yalco Formation (YF)

YF Facies 1

The Yalco formation is characterised by dolomite, phengite, phengitic illite and ankerite in the SWIR spectrum. The TIR spectrum shows predominantly silica, carbonate and potassium feldspar. Albedo is in the high range and overall core colour is light grey.

Bukulara Sandstone (BS)

BS Facies 1

Characterised by muscovite and kaolinite in the SWIR spectrum and almost solely silica in the TIR spectrum. There is a very high albedo for this facies which reflects the almost white core colouration. The gamma count is not outstanding in comparison to the average over the well interval.

BS Facies 2

The absence of kaolinite and a slightly lower average albedo are the only factors that separate this facies from facies 1 with the boundary between the two facies marked by a sharp dip in albedo.

4.2 Summary

The following table gives a more graphical representation of the characteristics of each of the HyLog facies identified from the interpretation. Gamma and albedo are given a descriptor which refers to the values in the table below:

Gamma Log Descriptors:	
Low	~350cps
Medium	~400cps
High	~450cps
Very High	~500cps
Albedo Descriptors:	
Very Low	0 - 0.15
Low	0.15 - 0.3
Medium	0.3 - 0. 45
High	0.45 - 0.6

Formation	Facies	SWIR	TIR	Albedo	Core Colour	Gamma
Mara Dolomite	1	Ankerite, Dolomite	Silica, Carbonate	Low	Dark Grey	-
Mitchell Yard Member	1	Aspectral, Muscovite, Ankerite, Dolomite	K-Feldspar	Low	Dark Grey	-
Teena Dolomite	**1**	Ankerite, Dolomite	Silica, Carbonate	Low	Dark Grey	-
	2	Dolomite	Carbonate, K-Feldspar	Medium	Light Grey	-
	3	Dolomite	Carbonate	Low	Dark Grey	Low
Coxco Dolomite	**1**	Ankerite, Dolomite	Carbonate	Medium	Light Grey / Cream	-
W-Fold Shale	1	Ankerite, Calcite, Chlorite-FeMg, Phengitic Illite	Carbonate, Silica, K-Feldspar, White-Mica, Sulphate, Chlorite	Medium	Light grey	Medium
	2	Dolomite	Carbonate, K-Feldspar	Medium	Light Grey	-
HYC Pyritic Shale	1	Gypsum, Aspectral	Sulphate, Silica, K-Feldspar, Invalid, White-Mica	Very Low	Black	Medium
Cooley Dolomite	1	Dolomite	Silica, Carbonate	Medium	White – Light Grey	-
Barney Creek Formation	1	Phengite, Phengitic Illite	Silica, K-Feldspar, Sulphate, White-Mica, Chlorite	Medium	White - Light Grey	Medium
	2	Phengite, Ankerite, Dolomite , Muscovite	Invalid, Carbonate, Silica	Low	Dark Grey	Medium

Formation	Facies	SWIR	TIR	Albedo	Core Colour	Gamma
	3	Phengite, Aspectral, Gypsum, Ankerite, Dolomite	Sulphate, Silica, K-Feldspar, Carbonate	Low	Dark Grey	Low
	4	Phengite, Aspectral, Gypsum	Sulphate, Silica, K-Feldspar, Carbonate	Low	Red - Brown	Low
	5	Phengite, Muscovite, Aspectral, Ankerite,	Silica, K-Feldspar	Medium	Light Grey	Low
	6	Phengite, Aspectral, Gypsum, Muscovite	Sulphate, Silica, K-Feldspar, Carbonate	Very Low	Dark Grey - Black	
	7	Ankerite, Dolomite, Aspectral, Muscovite	Silica, K-Feldspar, Carbonate, Plagioclase	Low	Dark Grey	-
	8	Aspectral	Silica, K-Feldspar, White-Mica, Carbonate, Sulphate, Plagioclase	Very Low	Black	-
	9	Phengite, Ankerite, Dolomite, Aspectral, Jarosite	Silica, K-Feldspar, White-Mica, Carbonate, Sulphate, Plagioclase		Dark Grey	-
	10	Ankerite, Dolomite, Aspectral, Gypsum	Carbonate, Silica, K-Feldspar, Sulphate, Invalid			Medium
	11	Aspectral, Gypsum	White-Mica, Silica, Sulphate	Low	Black (mottled)	Medium

Formation	Facies	SWIR	TIR	Albedo	Core Colour	Gamma
	12	Ankerite, Dolomite, Gypsum, Muscovite	Silica, K-Feldspar, Carbonate, Sulphate, Plagioclase, White-Mica,	Low	Light Grey	Medium
Surprise Creek Formation	1	Ankerite, Dolomite, Gypsum, Aspectral	Carbonate, Silica, K-Feldspar, Sulphate,	Low	Dark Grey	High
	2	Ankerite, Dolomite, Aspectral	Carbonate,	Medium	Light Grey	Medium
Reward Dolomite	1	Phengite, Ankerite, Dolomite	Silica, Carbonate	Medium	Light Grey	High
	2	Ankerite, Dolomite, Aspectral	Silica, Carbonate, Sulphate,	Medium	Light Grey	Low
	3	Ankerite, Dolomite, Gypsum, Aspectral Muscovite	Silica, Carbonate	Medium	Brown	High
Lynott Formation	1	Phengite, Dolomite	Silica, K-Feldspar, White-Mica, Smectite, Carbonate	High	Light Brown	Very High
	2	Phengite, Dolomite, Muscovite,	Carbonate, Silica, Sulphate	High	Light Brown	High
	3	Aspectral, Ankerite, Gypsum, Dolomite	Silica, K-Feldspar, White-Mica, Smectite, Carbonate, Invalid	Medium	Dark Brown / Grey	High

	4	Aspectral, Gypsum	White-Mica, Sulphate, Silica	Low	Black / red with white mottling	High
Caranbirini Member	1	Dolomite, Phengite, Ankerite, Jarosite	Silica, Carbonate, K-Feldspar	Medium-High	Light Grey	-
Hot Springs Member	1	Dolomite, Phengite, Phengitic Illite, Ankerite, Chlorite-FeMg, Jarosite	Silica, Carbonate, K-Feldspar, Chlorite	Medium	Dark Grey	-
Hot Springs Member	1	Dolomite, Phengite, Phengitic Illite, Ankerite, Chlorite-FeMg, Jarosite	Silica, Carbonate, K-Feldspar,	Medium	Dark Grey	-
Yalco Formation	1	Dolomite, Phengite, Phengitic Illite, Ankerite	Silica, Carbonate, K-Feldspar	High	Light Grey	-
Bukulara Sandstone	1	Kaolonite,-WX, Muscovite, Phengite	Silica, White-Mica	Very High	Light Brown/Grey	Low
	2	Phengite	Silica	High	Brown	-

5 Petroleum Well Interpretation

5.1 Unit Description

Each unit will be described in terms of its wireline log, XRF and TOC data characterisitcs beginning with the oldest. Glyde-1 intersects the Bukulara Sandstone, Barney Creek Formation, the Cooley Dolomite and the Coxco Dolomite. Lamont Pass 3 intersects the undivided Lynott Formation, Reward Dolomite, Barney Creek Formation, Coxco Dolomite and the oldest formation; the Myrtle Shale.

Myrtle Shale (MS)

Unit 1

The Myrtle Shale is characterised by chaotic gamma and sonic logs that, on average, intermediate when compared to the rest of the well. It is difficult to divide into separate units due to the lack of XRF data for the interval which it covers in Lamont Pass 3 (Figure 4.1.2).

Coxco Dolomite (CX)

Unit 1

The Coxco Dolomite is a thick unit with the same wireline log characteristic as the Cooley Dolomite. All XRF plots show low concentrations aside from calcium oxide which is approximately 40%.

Barney Creek Formation (BC)

Unit 1

At the boundary of the overlying Bukulara Sandstone in Glyde-1 there is a significant decrease in silica to 50%, however gamma remains the same. There is also an increase in calcium oxide (CaO), which is an indicator of carbonate percentage, from zero to 10%. TOC carbon averages approximately 1.5% for this unit.

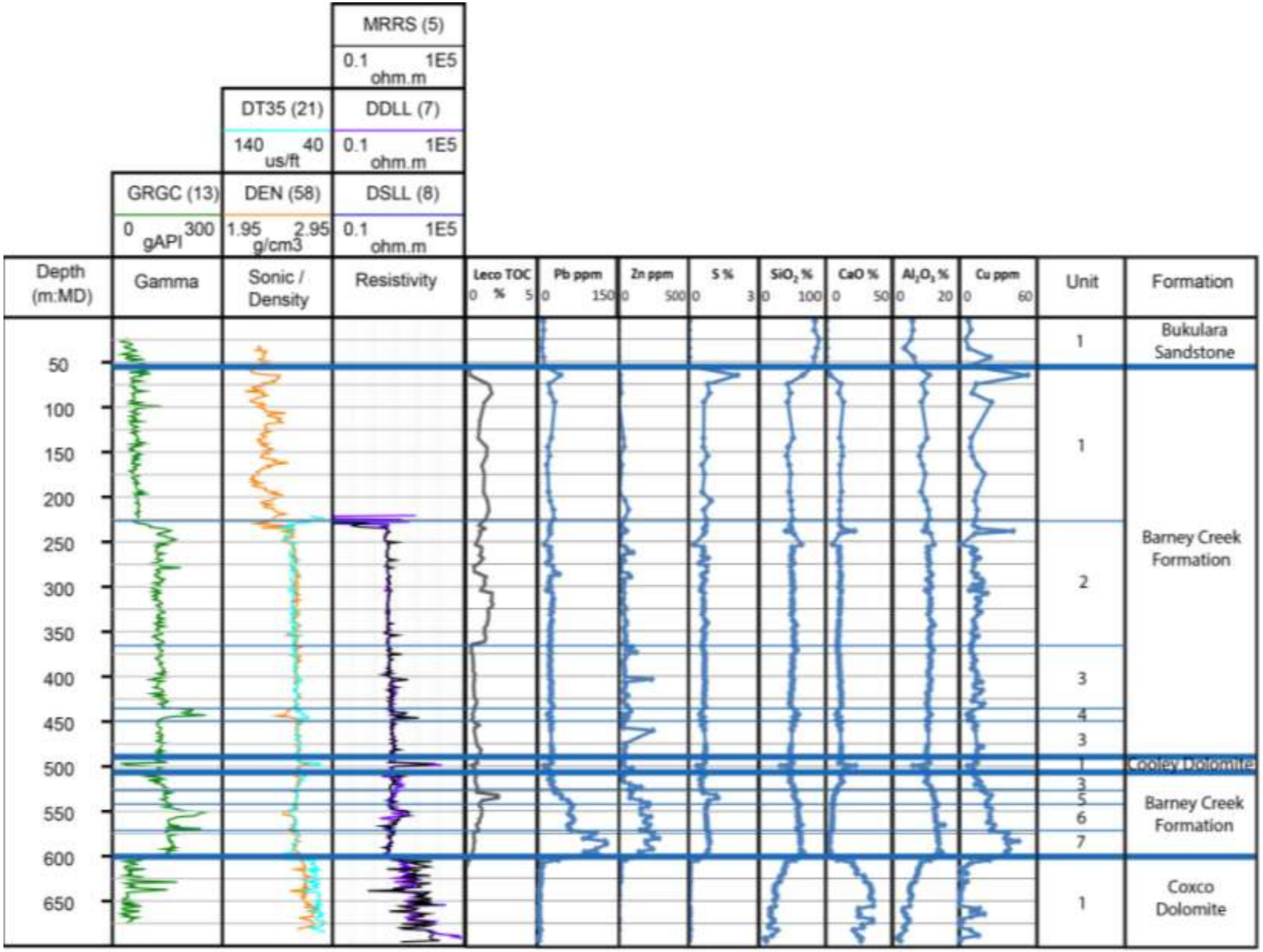

Figure 5.1.1 – Glyde-1 Wireline log, TOC and XRF Facies Interpretation.

Unit 2

This unit is segregated from unit 1 by an increase in the gamma count to about 150gAPI aswell as a slight increase in the density reading. Sonic and resistivity data is available for this interval with the sonic log measuring approximately 70µs/ft and the resistivity log averaging 30ohm/m.

Unit 3

This unit is identical to unit 2 aside from a drop in TOC from 1.5% to 0.5%.

Unit 4

Easily distinguishable in Glyde-1 (Figure 4.1.1) due to a peak in the gamma log and significant drop in density compared to the surrounding units. Resistivity also peaks at approximately 1000ohm/m while XRF data doesn't suggest any notable variation from unit 3.

Unit 5

Highlighted by a sharp TOC peak in Glyde-1 (Figure 4.1.1) of 2.5%, which is the highest for the entire well interval. There is also a corresponding minor peak in the sulphur XRF plot.

Unit 6

Consists of two outstanding gamma peaks which correspond with drops in both the density and sonic logs.TOC and XRF plots don't show any significant changes from the surrounding units.

Unit 7

This unit has the same wireline log signatures as unit 3 but has significantly different XRF data. The XRF plots show much higher concentrations of lead (Pb), zinc (Zn) and copper (Cu).

Unit 8

Relatively low gamma, in the order of 100gAPI and a high sonic reading of about 50µs/ft. Resistivity also quite high, averaging slightly above 1000ohm.m. The most outstanding XRF plot is the calcium concentration which sits at about 15% over this unit.

Unit 9

Slightly lower calcium levels for this unit in comparison to the overlying unit 9 in Lamont Pass 3 (Figure 5.1.2) Copper concentration appears to spike in this unit reaching a maximum of nearly 200ppm. Otherwise wireline logs show similar trends as before with only a slightly higher average gamma value.

Unit 10

Characterised by an almost zero gamma reading and low concentrations in all XRF plots besides having the peak calcium content for the well of 20%.

Unit 11

This unit has the highest overall gamma count for the well with an average of approximately 400gAPI. The sonic log shows a reading slightly lower in comparison to the rest of the Barney Creek in Lamont Pass 3 (Figure 5.1.2) Phosphorous peaks at 2500pm while the calcium concentration drops to 10%.

Unit 12

Probably the most noticeable unit of the Barney Creek Formation within Lamont Pass 3 (Figure 5.1.2). The sonic log shows a consistent 45µs/ft and resistivity is the lowest within the well reaching 10ohm/m. This corresponds with high concentrations of sulphur (S), iron (Fe), manganese (Mn) and lead (Pb).

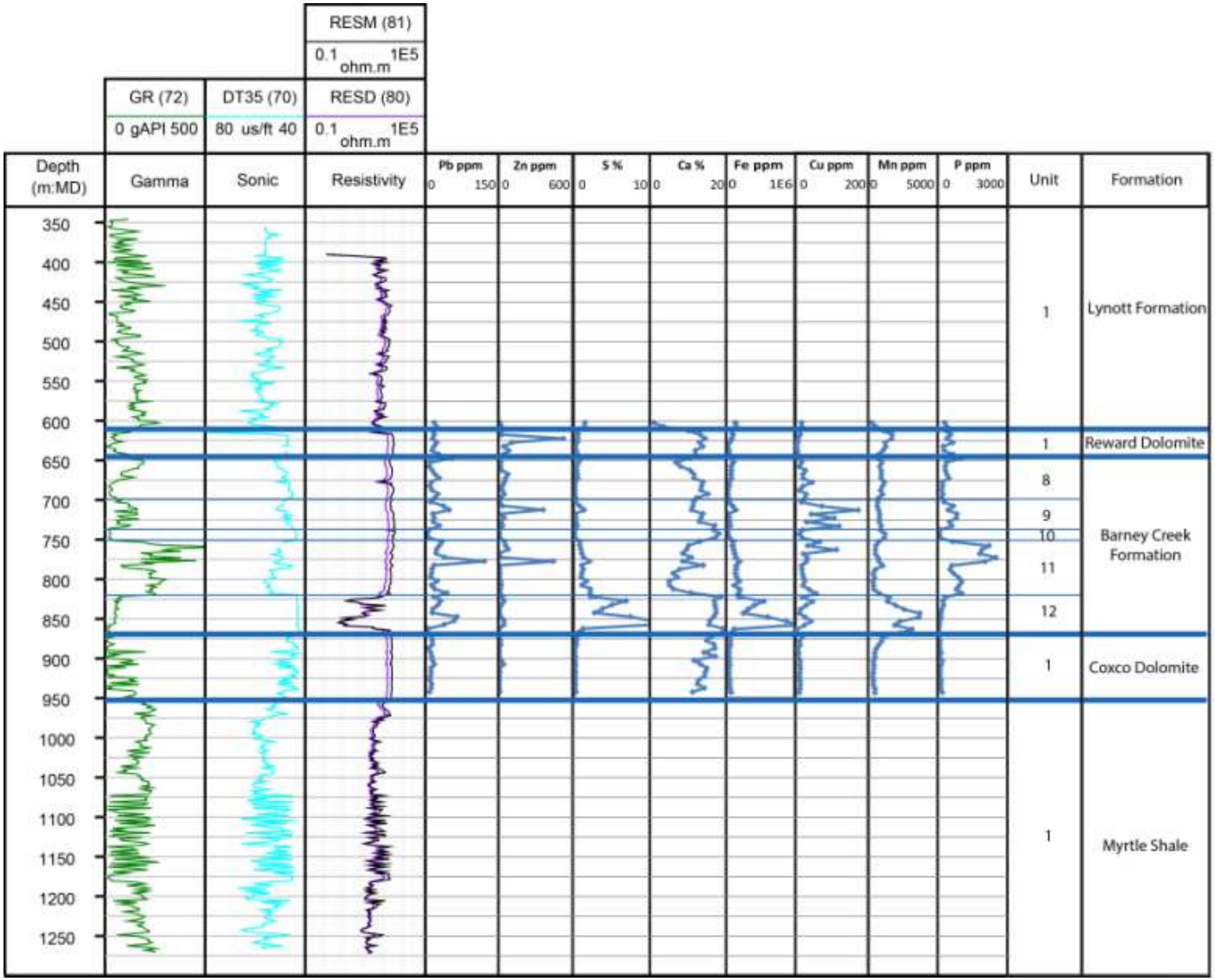

Figure 5.1.2 – Lamont Pass-3 Wireline log, TOC and XRF Facies Interpretation.

Cooley Dolomite (CD)

Unit 1

A very thin unit in Glyde-1 (Figure 4.1.1) characterised by a sharp drop in gamma count to almost zero and corresponding peaks in the sonic, density and resistivity logs. XRF ploys show an increase in calcium oxide and decrease in alumina and silica concentrations.

Reward Dolomite (RD)

Unit 1

Characterised by very low gamma and high average sonic and resisitivity values. Unsurprisingly, the calcium concenration is prominent at 15% and there is also appears to be a peak in zinc concentrations.

Lynott Formation (LF)

Unit 1

The Lamont Pass 3 (Figure 5.1.1) wireline logs show a low chaotic gamma and high sonic reading for the Lynott formation. Resistivity is also high and averages about 1000 ohm.m. There is no XRF data available for this interval which makes further differentiation difficult.

Bukulara Sandstone (BS)

Unit 1

Unsurprisingly, the silica content for this unit is almost 100% and the gamma count is low. The XRF data also shows approximately 5% alumina (Al_2O_3) and minor copper concentration. Density is low in comparison to the rest of the interval with an average of about 2.25 g/cm^3 and no sonic or resistivity data is avaliable for this unit. Total organic carbon (TOC) is zero over the entire unit.

5.2 Summary

The following table gives a more graphical representation of the wireline and TOC characteristics of each of the units identified from the interpretation of the petroleum well data. Gamma, sonic, density, resistivity and TOC are given a descriptor which refers to the values in the table below:

Gamma Log Descriptors:	
Low	0-100gAPI
Medium	100-250 gAPI
High	250-500gAPI
Sonic Log Descriptors:	
Low	100-140µs/ft
Medium	60-100µs/ft
High	40-50µs/ft
Density Log Descriptors:	
Low	1.95-2.25g/cm^3
Medium	2.25-2.75g/cm^3
High	2.75-2.95g/cm^3
Resistivity Log Descriptors:	
Low	0 - 10 ohm.m
Medium	10 – 1000ohm.m
High	1000 - 100000 ohm.m
TOC Log Descriptors:	
Low	0-1%
Medium	1-2%
High	2-5%

Formation	Unit	Gamma	Sonic	Density	Resistivity	TOC
Myrtle Shale	1	Medium	Medium	-	High	-
Coxco Dolomite	1	Low	High	High	High	Low
Cooley Dolomite	1	Low	High	High	High	Low
Barney Creek Formation	1	Low	-	Medium	-	Medium
	2	Medium	Medium	High		Medium
	3	Medium	Medium	High		Low
	4	High	Medium	Medium		Low
	5	Medium	Medium	High		High
	6	High	Low	Medium		Low
	7	Medium	Medium	High		Low
	8	Low	High	-		-
	9	Medium	High	-		-
	10	High	Medium	-		-
	11	Low	High	-		-
	12	Low	High	-	Low	-
Lynott Formation	1	-	High	-	Medium	-
Bukulara Sandstone	1	Low	-	Medium	-	Low

6 Correlation

Figure 6 on the following page shows the correlation between the wireline and TOC data of Glyde-1 and the HyLog and core photo tracks from Glyde-9. It is important to note that the depth scales are not the same as the purpose of the figure is to illustrate the relationship between the petroleum well and mineral data as opposed to differences in thicknesses.

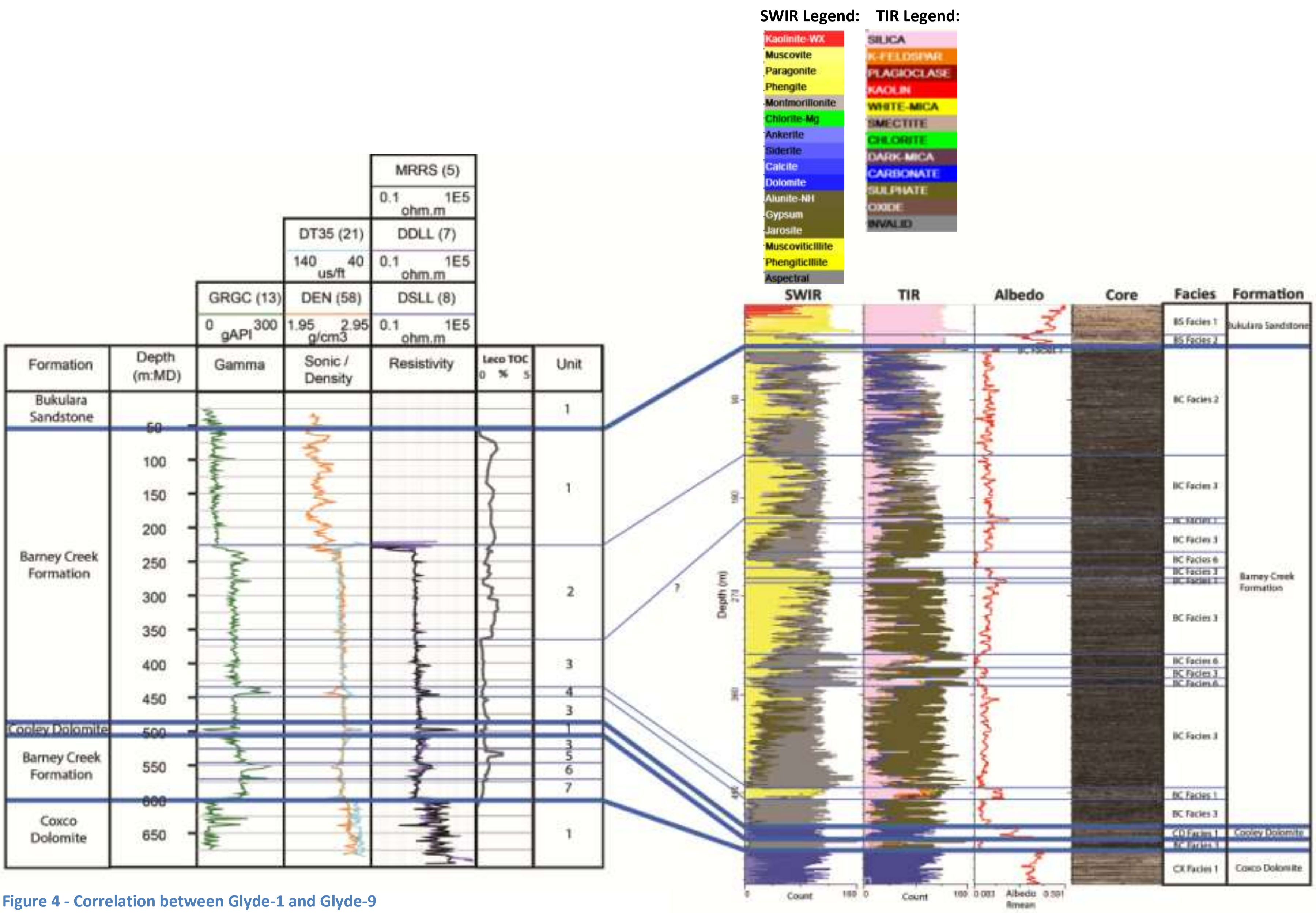

Figure 4 - Correlation between Glyde-1 and Glyde-9

7 Discussion

7.1 Depositional Environments

In general, formations which are largely comprised of dolomite in the SWIR spectrum such as the Mara Dolomite, Teena Dolomite, Coxco Dolomite, Cooley Dolomite and Reward Dolomite appear identical from the mineral well data. This indicates that these facies probably share a similar depositional environment or that, in the case of the Cooley Dolomite, the formation is derived from an older one. TD Facies 1, RD Facies 2, MD Facies 1 and CD Facies 1 have a TIR spectrum consisting of only carbonates and silica. Such a composition is indicative of a shallow saline marine environment which experiences regular influxes of sand. This could be in the form of a marginal marine lagoon which is periodically connected with the ocean or a carbonate platform similar to that presented in Figure 2.1.2. The fact that CD Facies 1 shares mineralogical characteristics with TD Facies 1 and MD Facies 1 supports the claim of Jackson et al. (1987) that the Cooley Dolomite is a product of the Teena Dolomite and Emerugga Dolomite, of which the Mara Dolomite is a member. This relationship is probably a result of erosion of the earlier facies and re-deposition in a slump structure as shown in Figure 2.1.3. Other dolomitic facies such as TD Facies 2, CX Facies 1 that have TIR spectrums showing solely carbonate are probably representative of saline lagoons or brine lakes that are isolated from external sedimentation as suggested by Davidson and Dashlooty (1993) instead of lacustrine setting favoured by Jackson et al. (1987)

The W-Fold Shale is in fact more of a carbonate as opposed to shale with abundant calcite and ankerite in the SIWR spectrum and carbonates dominating the TIR spectrum. This favours a hyper saline brine pool / tidal flat depositional environment as proposed for this unit by Davidson and Dashlooty (1993).

The HYC Pyritic Shale is only intersected by Myrtle 5 and is represented by an approximately 10m thick facies overlying the W-Fold Shale. The most defining feature of this facies is the black core colour which corresponds with an extremely low albedo and dominating aspectral mineralogy.

Gypsum and sulphates present are more likely to be the result of oxidation from pyrite and other sulphides. All of these attributes are suggestive of an anoxic environment such as a lake bottom or restricted lagoon as suggested by Logan and Williams (1984) (Figure 2.1.3).

The Barney Creek Formation Creek Formation is present in every well and consists of the most facies. The most recognisable is BC Facies 1 which is identified as volcanic tuffs; BC Facies 5 is also likely to be a volcanic tuff with a slightly variable composition to BC Facies 1. This would mean that there were two volcanic sources which is one of the conclusions of Davidson and Dashlooty (1993). The facies are coincident with BC facies 2, 3, 4 and 10 in Glyde-8 and 9 (Figure 4.1.5 and 4.1.4 respectively). and Myrtle 5 (Figure 4.1.2) which together comprise the Undivided Barney Creek Formation. On the whole, these facies can be divided into an upper carbonate rich group (BC Facies 2 and 10) and lower sulphate rich group (BC Facies 3, 4 and 6). Again, these sulphates are more than likely the oxidation product of sulphides after core removal. This group is probably representative of the deeper water facies described by Davidson and Dashlooty (1993) while the carbonate rich group tends to suggest relations with the shallow water depositional environment described. This tuffaceous portion of the Barney Creek Formation is probably akin to the section intersected by Glyde-1 (Figure 5.1.1) BC Units 4 and 6 have the expected wireline characteristics of a volcanic tuff with BC Unit 1 alike the carbonate rich upper group and the other units comprising the deeper water facies. Tuffs aren't present in Leviathan 9 (Figure 4.1.1) or Berjaya 2 (Figure 4.1.3). This is consistent with a southerly source as presented by Davidson and Dashlooty (1993) as these two wells are two of the most northerly wells, however, Myrtle 5 is positioned between them and does feature tuffs. BC Facies within Leviathan 9 and Berjaya 2 are not observed in any of the other three wells. This suggests that the section of Barney Creek Formation seen in Glyde-1, 8 and 9 and Myrtle 5 was either not deposited at the Leviathan 9 and Berjaya 2 localities or was eroded after deposition. The presence of tuffs in Myrtle 5 makes erosion the more likely option as it is assumed that ash would have at least been deposited in Leviathan 9 which is more proximal to the source than Myrtle 5. In general, the section of the Barney Creek Formation in Leviathan 9 and Berjaya 2 (BC Facies 7, 8, 9 and 12) show similar composition but much different abundances in comparison to the Undivided Barney Creek Formation in other wells. The most obvious difference is that these facies are much more silica rich. This could be an indication that these sediments have been reworked which may have obliterated the thin volcanic tuff signatures that were previously present. These facies could be comparable with BC Unit 8, 9, 10 and 11 in Lamont Pass 3 (Figure 5.1.2) which are also vastly different from the Undivided Barney Creek Formation in Glyde-1 (Figure 5.1.1) BC Unit 12 is unique to Lamont Pass 3 and is a brecciaed portion of the Undivided Barney Creek Formation which is probably associated with movement along the Emu Fault which the well is situated on.

The Yalco formation (YF Facies 1) and members of the Lynott Formation (LF Facies 1,2,3,4 HS Facies 1 and CM Facies 1) have similar HyLog signatures and a conformable contact which suggests these formations may have been deposited in the same or very similar depositional environments. It is hard to discern from the HyLog data alone but the interpretation of Muire et al. (1980) of an ephemeral lake does not seem unreasonable as seasonal variations in water fall/level this could explain the fluctuations in abundances of carbonates and silica. The gamma log in Lamont Pass 3 (Figure 5.1.2) offers no assistance and fluctuations in the density log probably reflects alternation between silica rich sections and the denser carbonate rich sections.

7.2 Thicknesses and Distribution

Thickness and distribution of sediment packages is largely controlled by accommodation space, sediment supply and erosion. The most obvious evidence for erosion is where the Cambrian Bukulara Sandstone directly overlies Paleoproterozoic upper McArthur Group formations. This occurs In Glyde-8, Glyde-9, Leviathan 9 and Glyde-1 (Figures 4.1.1, 4.1.2, 4.1.3 and 5.1.1). Within the Glyde Sub-basin there appears to have been more significant erosion as the Bukulara Sandstone sits directly on top of the Barney Creek Formation in Comparison to Leviathan 9 where a portion of the Yalco Formation remains.

Despite evidence suggesting that partial erosion of the Barney Creek Formation may have occurred within the Glyde Sub-basin there is still a significantly thicker section (up to 550m) in the basin in comparison to elsewhere in the study area. This observation supports the assertions of Davidson and Dashlooty (1993) that the Glyde- Sub basin contains the thickest section of the Barney Creek Formation. Another key observation is that Glyde-8 contains a 50m thicker section of Barney Creek Formation than Glyde-1 and Glyde-9 which also supports Davidson and Dashlooty's (1993) claim that Block 7 (where Glyde-1 and Glyde-9 are situated; Figure 2.2.2) is a paleo-high and was possibly a horst. It is notable that the W-Fold Shale is present in Glyde-8 and none of the other wells situated in the Glyde Sub-basin.

Moving outside of the Glyde Sub-basin, the thickness of the Barney Creek Formation becomes drastically thinner despite conformal contacts with the overlying units suggesting less erosion has taken place in these structural domains. This has to then be associated with limited accommodation space in comparison to the Glyde Sub-basin.

While the Undivided Barney Creek Formation is present in all wells the W-Fold Shale is only intersected by two wells and the HYC Pyritic Shale by a single well. A 10m section of the W-Fold Shale occurs at the bottom of Glyde-8 in addition to a 40m section in Myrtle 5 while a 10m portion of the HYC Pyritic Shale only features in Myrtle 5. The fact that these members occur outside of the Barney Creek Formation probably implies that they are not dependent on accommodation space and rather, the right depositional environment.

7.3 Relationships between Mineral and Petroleum Well Data

Correlation between Glyde-1 and Glyde-9 allows connections to be drawn between mineral and petroleum well data. These wells were chosen as they are in close proximity to one another and within the same structural domain which makes for the most direct and accurate correlation. Despite this being the case, there are still variations in unit thicknesses most notably in the section of the Barney Creek Formation underlying the Cooley Dolomite in each well. This highlights the lateral variability in accommodation space / sedimentation rates associated with a depositional environment as previously discussed (Figure 2.1.5) Nevertheless, there are still a number of important relationships that can be taken from the correlation.

It would appear from that only tuffs with a significant thickness create a response in the wireline logs, particularly in the gamma and density logs. This makes for difficulty in judging the accuracy of correlations as tuffs are a usual tool since they represent a single period in time.

Initially it was thought that aspectral mineralogy may correspond with zones of high TOC however correlation suggests this is not the case as the entire Undivided Barney Creek Formation has abundant aspectral mineralogy whereas the whole section does not have high TOC (Figure 6). Instead it is proposed that zones of high TOC correspond well with invalid mineralogy in the TIR spectrum. If this is true then the suggested correlation marked '?' would be definite (Figure 6). Another reason for this suggestion is that the supposed 'sweet spot' in terms of TOC in the HYC Pyritic Shale also has invalid mineralogy prevalent in the TIR spectrum.

7.4 Applications for Petroleum Exploration

Understanding the relationship between mineral well data and petroleum well data has numerous potential benefits for petroleum exploration in areas such as the McArthur Basin. For a petroleum exploration company mineral well data in an area is basically free information and by learning how to apply this data to the petroleum industry could result in significant savings.

For example, if the relationship between TOC rich zones and invalid mineralogy on HyLogs proved true the abundance of TOC data becomes much more widespread in areas such as the McArthur Basin where mineral wells are abundant. This allows for more accurate reservoir mapping and identification of 'sweet spots' which is a key factor for producing unconventional petroleum.

8 Conclusions and Recommendations

8.1 Conclusions

There is no question that the various structural domains (Figure 2.3) are related to accommodation space and uplift/erosion trends which determine the thickness of formations. However, there doesn't appear to be any connection between depositional environments and their associated facies with these structural domains (Figure 2.3). This is probably to be expected as each structural domain has complexities within itself as shown in Figure 2.1.5 which have an effect on water depth, accommodation space and sedimentation rate. This results in lateral facies changes which make predicting the location of specific facies, such as the HYC Pyritic Shale, very difficult. However, there is much to be gained through incorporating mineral well data into a petroleum exploration program.

8.2 Recommendations

Further research should be directed at testing the proposed relationship between HyLog data and TOC content as this would be the most beneficial relationship to establish. Also, further study on the relationship between handheld gamma data from core versus wireline gamma data could prove useful as the handheld gamma data used does not appear to show the trends expected from wireline gamma data of similar facies.

References

Brown M.C., Claxton, C.W. Plumb, K.A. (1969): The Proterozoic Barney Creek Formation and some associated carbonate units of the McArthur group, Northern Territory, BMR Record, 1969/145

Bull S.W. (1998): Sedimentology of the Palaeoproterozoic Barney Creek formation in DDH BMR McArthur 2, southern McArthur basin, northern territory, Australian Journal of Earth Sciences: An International Geoscience Journal of the Geological Society of Australia, 45:1, 21-31

Crick I.H., Boreham C.J., Cook A.C. & Powell T.G. (1998): Studies on petroleum geology and geochemistry of the Middle Proterozoic McArthur Basin, Northern Australia II, Assessment of source rock potential: American Association of Petroleum Geologists Bulletin, 72, 1495-1514.

Davidson G.J. & Dashlooty S.A. (1993): The Glyde Sub-basin: A volcaniclastic-bearing pull-apart basin coeval with the McArthur River base-metal deposit, Northern Territory, Australian Journal of Earth Sciences: An International Geoscience Journal of the Geological Society of Australia, 40:6, 527-543.

Dashlooty S.A. & Davidson G.J. (1986): Evolution of the Carpentarian Glyde River Sub-basin, McArthur Basin, NT, Geological Society of Australia Abstracts, 15, 54.

Jackson M.D., Sweet I.P. & Powell T.G. (1988): Studies on petroleum geology and geochemistry of the Middle Proterozoic McArthur Basin, Northern Australia I, Petroleum potential, Australian Petroleum Exploration Association Journal, 28, 283-302.

Logan R.G & William S.N. (1984), Sedimentary controls on the hydrothermal system that formed the HYC deposit at the McArthur River, Northern Territory, Geological Society of Australia, Abstracts15, 399.

Muir, M. D., Armstrong, K. J., & Jackson, M. J., (1980a)— Precambrian hydrocarbons in the McArthur Basin, NT. BMRJournal of Australian Geology & Geophysics, 5, 301-304.

Muir, M. D., Lock, D., & Von der Borch, C. C., (1980b) The Coorong—model for penecontemporaneous dolomite formation in the Middle Proterozoic McArthur Group, Northern Territory, Australia. In Zenger, D. H., Concepts and models of dolomitization—their intricacies and significance. Society for Economic Paleontologists and Mineralogists, Special Publication28, 51-67.

Page, R.W., (1981) Depositional ages of the stratiform base metal deposits at Mount Isa and McArthur River, Australia, based on U-Pb zircon dating of concordant tuff horizons, Economic Geology, 76, 648-658.

Pietsch B. A., Rawlings D. J., Creaser P. M. et al. (1991) Bauhinia Downs 1:250 000 geological map series. Northern Territory Geological Survey Explanatory Notes SE53-3.

Plumb, K. A., & Brown, M. C, (1973) Revised correlations and stratigraphic nomenclature in the Proterozoic carbonate complex of the McArthur Group, Northern Territory. In Geological papers 1970-71. Bureau of Mineral Resources, Australia, Bulletin 139, 103-115.

Plumb K. A. (1979) The tectonic evolution of Australia. Earth Science Reviews 14, 205–249.

Plumb K. A. & Wellman P. (1987) McArthur Basin, Northern Territory: mapping of deep troughs using gravity and magnetic anomalies. BMR Journal of Australian Geology & Geophysics 10, 243–251.

Plumb K. A. (1987) Proterozoic extension and mineralisation in the McArthur Basin, Northern Territory, Australia. In: Applied Extension Tectonics, Extended Symposium Abstracts, pp. 72–79.

Plumb K. A., Ahmad M. & Wygralak A. S. (1990) Mid-Proterozoic basins of the North Australian Craton; regional geology and mineralisation. In: Hughes F. E. ed. Geology of the Mineral Deposits of Australia and Papua New Guinea, Vol. 1, pp. 881–902.

Plumb K. A. (1994) Structural evolution of the McArthur Basin, NT. In: 1994 AusIMM Annual Conference, Australian Mining Looks North; the Challenges and Choices, pp. 139–145. Australasian Institute of Mining and Metallurgy Publication Series 5/94.

Rawlings, D. J. (1999): Stratigraphic resolution of a multiphase intracratonic basin system: The McArthur Basin, northern Australia, Australian Journal of Earth Sciences, 46: 5, 703 — 723

Smith B. & Schmid S., (2014) Correlation between HyLoggerTM data and sedimentology across the McArthur Basin – Phase 1, NTGS, AGES Presentation, Alice Springs Convention Centre.

Walter, M. R., (1976) Stromatolites, Developments in Sedimentology, 20, Elsevier, Amsterdam.